

Terrace formation linked to outburst floods at the Diexi palaeo-landslide dam, upper Minjiang River, eastern Tibetan Plateau

Jingjuan Li¹, John D. Jansen², Xuanmei Fan¹, Zhiyong Ding¹, Shugang Kang³, Marco Lovati¹

¹ State Key Laboratory of Geohazard Prevention and Geoenvironment Protection, Chengdu University of Technology, Chengdu 610059, China

² GFÚ Institute of Geophysics, Czech Academy of Sciences, Prague, Czechia

³ State Key Laboratory of Loess and Quaternary Geology, Institute of Earth Environment, Chinese Academy of Sciences, Xi'an 710061, China

Correspondence to: John D. Jansen (j dj@ig.cas.cz); Xuanmei Fan (fxm_cdut@qq.com)

10 **Abstract**

River terraces are frequently investigated with the aim of extracting information regarding tectonic or climate forcing on the evolution of landscapes. Terraces formed following the blockage of valleys by large-scale landsliding have received limited attention despite the high likelihood of their prevalence in landslide-dominated mountain belts. Here, we investigate the geomorphology, sedimentology, and chronology of two outstanding sets of terraces upstream of the giant, river-blocking Diexi palaeo-landslide on the upper Minjiang River, eastern Tibetan Plateau. The first set occurs at Tuanjie village and has seven levels (T1-T7); the second set, at Taiping village, has three levels (T1-T3). All the terraces display a consistent sedimentary sequence comprising lacustrine muds topped by fluvial gravels sometimes capped by loess and a palaeosol. Based on field examination, lithofacies analysis, elevation data, and chronometric data (optically stimulated luminescence and radiocarbon dating), we correlate T1, T2 and T3 at Taiping with T5, T6 and T7 at Tuanjie. Our analysis suggests two damming and three outburst events have occurred at the Diexi palaeo-landslide over the past 35,000 years. A giant landslide (>300 m high) blocked the river before 35 ka followed by the first outburst flood at ~ 27 ka; the river was blocked again between 27 to 17 ka followed by a second outburst at ~17 ka; and a third outburst at ~12 ka was followed by gradual fluvial incision of the palaeo-dam crest to its current level. We attribute the terraces at Diexi to the recurrent blockage and outburst events, which reflect the shifting sediment transport capacity and incision at the palaeo-dam crest. Here, climatic fluctuations play a minor role in terrace formation, and tectonism plays no role at all.

1 Introduction

30 River terraces are temporary sediment storages along valleys that provide a natural archive of information on sediment transport and deposition through time (Chen et al., 2020; Liu et al., 2021), processes that are typically sensitive to the impacts of tectonism and climate (Pan et al., 2003; Singh et al., 2017; Aysin et al., 2019; Gao et al., 2020; Do Prado et al., 2022). Terraces have been shown to reflect a wide range of geomorphic controls, such as rock uplift rate (Jansen et al., 2013; Pan et al., 2013; Giano and Giannandrea, 2014; Malatesta et al., 2021), fault activity (Caputo et al., 2008), crustal flexure (Yoshikawa et al., 1964; Westaway and Bridgland, 2007; Okuno et al., 2014), glacier melting (Bell, 2008; Oh et al., 2019; Vásquez et al., 2022), changes in sediment supply (Jansen et al., 2011), sea level (Yoshikawa et al., 1964; Malatesta et al., 2021), and even the internal dynamics of the fluvial system (Schumm and Parker, 1973). In tectonically-active mountains, large-scale landslides, debris flows and 40 rockfalls (Molnar et al., 1993; Molnar and Houseman, 2013; Srivastava et al., 2017) can cause river blockages and associated sudden outburst floods that have a major impact on the sedimentary processes of the upstream and downstream reaches, including terrace formation (Korup et al., 2007; Hewitt et al., 2008; Korup et al., 2010; Hewitt et al., 2011). And yet, few studies have explored the influence of extreme events on the formation and evolution of terraces (Montgomery et al., 2004; Yuan and Zeng, 2012; Zhu et al., 2013; Chen et al., 2016; Arzhannikov et al., 2018; Hu et al., 2018; Arzhannikov et al., 2020; Xu et al., 2020). We attempt to address that knowledge gap here.

Rapid uplift and climate change during the Quaternary have led to frequent extreme geomorphic events in the area drained by the Minjiang River at the eastern margin of the Tibetan Plateau (Gorum et al., 2011; Fan et al., 2017; 2018; Wu et al., 2019; Dai et al., 2021; Yang et al., 2021). The upper Minjiang, 50 for instance, displays many terrace sequences with origins that remain debated (Yang, 2005). But due to the lack of detailed sedimentological, chronological and geomorphological information, the role of extreme geomorphic events, such as landslides and outburst floods, are still being explored (Yang et al., 2003; Yang, 2005; Gao and Li, 2006; Zhu, 2014; Luo et al., 2019).

A set of outstanding terraces occur just upstream of the 300 m-high Diexi palaeo-landslide dam, one 55 of the largest, best-preserved, and longest-duration landslide-dammed lakes in a tectonically-active setting (Fan et al., 2019). The Diexi terraces (Fig. 1) have been examined by previous workers (Wang et al., 2005b; Yang et al., 2008; Fan et al., 2019), but a systematic analysis has yet to be conducted. A set of

terraces at the village of Tuanjie is thought to have resulted via repeated outburst floods from the Diexi palaeo-dammed lake between 30 and 15 ka—each terrace corresponding to a different outburst (Duan et al., 2002; Wang et al., 2005a; Wang, 2009; Zhu, 2014; Ma et al., 2018). At least two blockage events
60 have also been suggested (Yang, 2005; Yang et al., 2008) together with four periods of fluvial progradation (Xu et al., 2020). However, mechanistic details of the terrace formational processes based on the sedimentology and a comprehensive dating analysis are lacking. Here, we seek to address the unresolved questions of the origins of the Diexi terraces, including the following aims: (1) to conduct a
65 detailed analysis of terrace sedimentology; (2) to obtain absolute depositional ages of the terraces (at Tuanjie and Taiping); and (3) to understand the evolution of the Diexi palaeo-dam since its formation at more than 35 ka (Wang et al., 2020). Our broader objective is to provide a better understanding terrace formation linked to extreme geomorphic events in mountain regions.

2 Study area

70 The Diexi palaeo-landslide dam is located on the eastern Tibetan Plateau in the upper reaches of the Minjiang River. The area exposes rocks of the eastern part of the Bayan Har Block (Fig. 1a), spanning the Devonian, Carboniferous, Permian, Triassic, and Quaternary periods (An et al., 2008; Zhang et al., 2011; Ma, 2017; Zhong, 2017). This region of the Tibetan Plateau has been affected by intense and frequent earthquakes (Yang et al., 1982; Chen and Lin, 1993; Li and Fang, 1998; Shi et al., 1999; Hou et al., 2001; Lu et al., 2004) linked to the ongoing collision of the Indian and Eurasian plates (Fig. 1b).
75

The Diexi study has an arid to semi-arid climate (Shi, 2020), with a strong effect of the prevailing winds. Cumulative evaporation averages 1000–1800 mm/y (Yang, 2005), and mean temperature and precipitation are 13.4°C and 500–600 mm/y, respectively. Vegetation patterns show major elevational zonation and comprise mainly of mountain coniferous forests, alpine meadows, and low shrubs at the
80 highest elevations.

The Minjiang valley widens downstream, overall, varying from 60 to 300 m wide at the valley floor (Yang, 2005; Jiang et al., 2016; Ma, 2017; Zhang, 2019), and up to 3000 m deep flanked by steep hillslopes that are typically 30–35° (Zhang et al., 2011; Guo, 2018). The Diexi palaeo-dammed lake (31°26′–33°16′ N; 102°59′–104°14′ E) is situated on the bend of the V-shaped Minjiang valley, which in
85 turn lies in the well-known ‘north-south earthquake tectonic zone’ (Tang et al., 1983; Huang et al., 2003;

Yang, 2005; Deng et al., 2013).

The Diexi palaeo-landslide is located on the left bank of the Minjiang River at Jiaochang village (Fig. 1b). The palaeo-landslide length and width are ~ 3500 m and 3000 m, respectively, and volume is ~ 1.4 to 2.0 km³ (Zhong et al., 2021). The highest parts of the palaeo-landslide reach up to 3390 masl (metres above sea level), whereas the elevation of the dam crest is ~ 2500 masl (Dai et al., 2023).

At Taiping village (32°12' N, 103°45' E), three terraces occur near the mouth of Luobogou Gully (Fig. 1d) (Wang et al., 2005a; Fan et al., 2021), while a suite of seven terraces occurs 12 km downstream at Tuanjie village (32°2' N, 103°40' E) near the mouth of the Songpinggou tributary (Fig. 1c). Further downstream, high-energy gravel outburst deposits occur at scattered locations, including near the villages of Xiaoguanzi, Shuigouzi, and Manaoding (Fig. 1b).

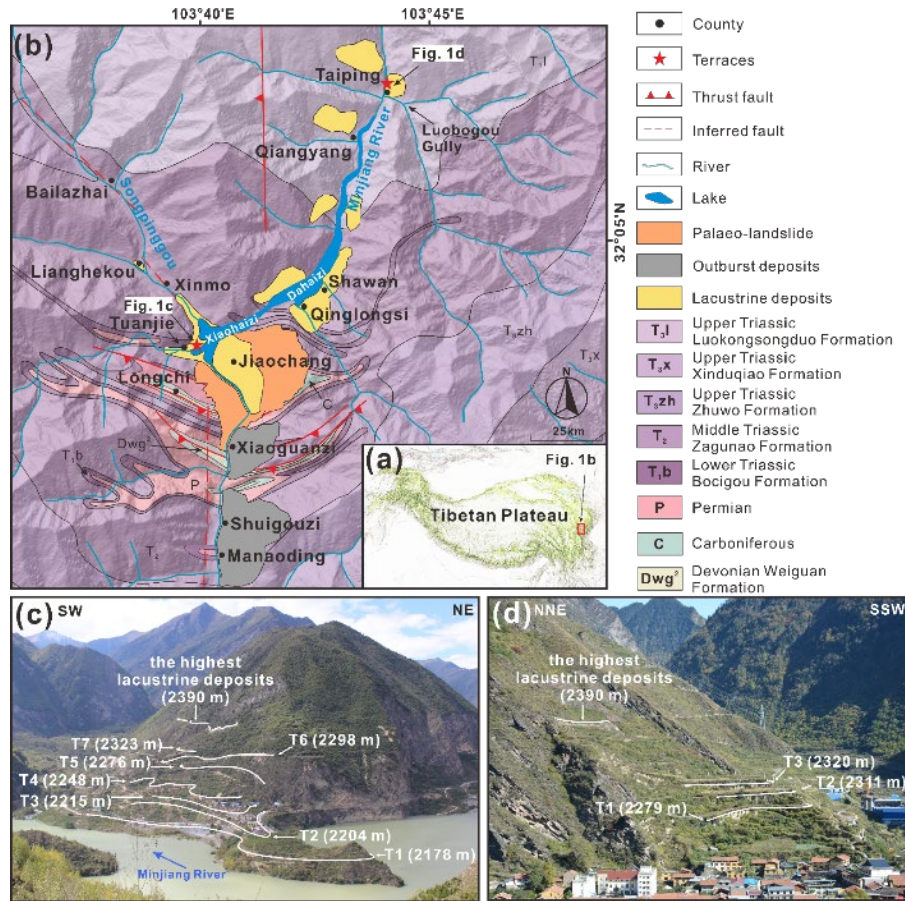


Figure 1. The Diexi study area. (a) Location of Diexi at the eastern margin of the Tibetan Plateau. (b) Geological setting (maps modified from Guo, 2018; Wang et al., 2020a; Zhong et al., 2021). (c) Oblique view of the seven Tuanjie terraces, including elevations (masl). (d) Oblique view of the three Taiping terraces including elevations (masl).

3 Materials and methods

3.1 Geomorphic and sedimentary description

Field surveys were carried out from October to November 2018. We described sedimentary structure, geometric shape, sorting, roundness, and palaeo-flow direction of the gravels by applying the lithofacies approach primarily based on Miall (2000), but also including previous work conducted by Yang (2005) and Yang et al. (2008) (Table. 1). The terraces were numbered according to elevation from the lowermost terrace (T1) to higher terraces (Tn).

Terrace elevations were measured using Light Detection And Ranging (LiDAR) data with ~ 0.5 m vertical accuracy and the Advanced Spaceborne Thermal Emission and Reflection Radiometer Global Digital Elevation Model (ASTER GDEM) with ~ 30 m vertical accuracy (Fan et al., 2021).

Table. 1 Lithofacies of terrace sediments at Diexi. Adapted from Miall (2000), Yang (2005) and Yang et al. (2008).

Lithofacies code	Lithofacies	Sedimentary structures	Interpretation
Ps	Palaeosol	Pedogenic features, roots	Pedogenesis
Ls	Sandy loess	Massive texture	Eolian deposits
Gmm	Matrix-supported, massive gravel	Weak grading	Plastic debris flow (high-strength, viscous)
Gh	Clast-supported, crudely bedded gravel	Horizontal bedding, imbrication	Longitudinal bedforms, lag deposits, sieve deposits
Gci	Clast-supported gravel	Inverse grading	Clast-rich debris flow (high strength), or pseudoplastic debris flow (low strength)
Gcm	Clast-supported, massive gravel	-	Pseudoplastic debris flow (inertial bedload, turbulent flow)
Fm	Mud	snail shells	Overbank, abandoned channel, or drape deposits
Fl	silty clay	parallel bedding, wave bedding	Lacustrine deposits

3.2 Chronology

Two independent dating methods: optically stimulated luminescence (OSL) and radiocarbon dating, were employed to establish a reliable chronostratigraphic framework for the Tuanjie and Taiping terraces. We collected samples from the top and bottom of the lacustrine units, the top of the gravel units, and from the base of the loess and palaeosol units with the aim of clarifying the timing of the damming and outburst processes and terrace stability: nineteen OSL samples and nine radiocarbon samples in total

(Figs. 2 and 3).

3.2.1 OSL dating

At the Tuanjie terraces, twelve samples were taken from the lacustrine deposits (excluding T6 and the highest lacustrine deposits); two samples were collected from the gravel units of T2 and T5, and samples were taken from palaeosols at T1 to T5 and T7 (Figs. 2 and 3). At the Taiping terraces, four samples were taken from the lacustrine deposits at T1 to T3 and the highest deposits, and another was taken from the palaeosol unit at the T3 (Figs. 2 and 3). Samples were collected from freshly dug exposures, inserting stainless steel tubes followed by careful sealing from light.

Samples were processed and measured at the Institute of Earth Environment, Chinese Academy of Sciences. The quartz grains were extracted following standard laboratory pre-treatment procedures (Kang et al., 2013; 2020). The sediment at the tube-ends, which may have been exposed to daylight during sampling, were discarded and the unexposed samples were prepared for equivalent dose (D_e) and environment dose rate determination. Approximately 50 g samples were treated with 30% HCl and 30% H_2O_2 to remove carbonates and organic matter, respectively. The samples were then washed with distilled water until the pH value of the solution reached 7. For samples IEE5542 and IEE5550, the coarse fractions (90-150 μm) were sieved out and etched with 40% HF for 45 mins, followed by washing using 10% HCl and distilled water. For the other 17 samples, the fine polymineral grains (4-11 μm) were separated according to the Stokes' law. These fine polymineral grains were immersed in 30% H_2SiF_6 for 3-5 days in an ultrasonic bath to extract quartz. Finally, the purified fine (coarse) quartz was deposited (mounted) on stainless steel discs with a diameter of 9.7 mm. The purity of quartz was verified by IRSL intensity and OSL IR depletion ratio (Figs. S1 and S2a; Duller, 2003).

All OSL measurements were performed on a Lesxyg Research measurement system, with blue light at (458 ± 10) nm, and infrared light at (850 ± 3) nm for stimulation and a $^{90}S/^{90}Y$ beta source (~ 0.05 Gy/s) for irradiation. Luminescence signals were detected by an ET 9235QB photomultiplier tube (PMT) through a combination of U340 and HC340/26 glass filters.

The single-aliquot regenerative-dose (SAR) protocol (Table. S1; Murray and Wintle, 2000; Wintle and Murray, 2006) was utilised to determine the Equivalent Dose (D_e) following Kang et al. (2020). Quartz grains were preheated at 260°C for 10 s for natural and regenerative-dose, and a cut-heat at 220°C for 10 s was applied for the test dose. The quartz was stimulated for 60 s at 125°C with blue LEDs; the

150 OSL signal was calculated as the integrated value of the first 0.5 s of the decay curve minus the integrated
value of the last 0.5 s as the background. For D_e determination, approximately 10 aliquots were measured
for each sample. The mean D_e value of all aliquots was used as the final D_e value. Conventional tests in
SAR protocol, including recuperation ratio, recycling ratio, quartz OSL brightness and fast-component
dominated nature, growth curve shape, and D_e distribution (Figs. S2 and S3), indicated that the protocol
155 is adequate for the samples in this study.

The environmental dose rate was estimated from the radioisotope concentrations (U, Th, and K) and
cosmic dose rates. U and Th concentrations were determined by inductively coupled plasma mass
spectrometry, while K concentration was measured by inductively coupled plasma optical emission
spectrometry. The cosmic dose rates were calculated using the equation proposed by Prescott and Hutton
160 (1994). The α -value of fine-grained (4-11 μm) quartz was assumed to be 0.04 ± 0.002 (Rees-Jones, 1995).
Considering the sedimentary texture, and current and past climate conditions since deposition, the water
content of the gravel and palaeosol was assumed to be $10 \pm 5\%$, while the water content of lacustrine
deposits was estimated to be $20 \pm 5\%$. Dose rate was calculated using the Dose Rate and Age Calculator
(DRAC) (Durcan et al., 2015). Finally, the quartz OSL ages were obtained by dividing the measured D_e
165 (Gy) by the environmental dose rate (Gy/ka).

3.2.2 Radiocarbon dating

Nine samples (all bulk sediment) were collected for radiocarbon analysis: two from the highest
lacustrine deposits in the Tuanjie and Taiping Terraces, one from the loess cap at Tuanjie T4, three from
the bottom lacustrine deposits at Tuanjie T2, and three from the bottom lacustrine deposits at Taiping T1,
170 T2, and T3 (Figs. 2 and 3). The radiocarbon sample collected from the highest lacustrine deposits at
Taiping was used to compare with the OSL sample (TP19-1) taken from the same position. The
radiocarbon samples collected from the highest lacustrine deposits at Tuanjie and the equivalent at
Taiping were compared. Utilising the same dating method for age comparison enhances the robustness
of our analysis. We sampled the loess unit at Tuanjie T4, as it was the most complete and easiest to access.
175 Six samples taken from the bottom lacustrine deposits were used to determine the depositional ages of
the terraces.

All samples were tested for organic matter, and analysed using the NEC accelerator mass
spectrometer and thermo infra-red mass spectrometer at the Beta Analytic Radiocarbon Dating

Laboratory. All radiocarbon ages reported here are calibrated using IntCal 20 (Reimer et al., 2020).

180

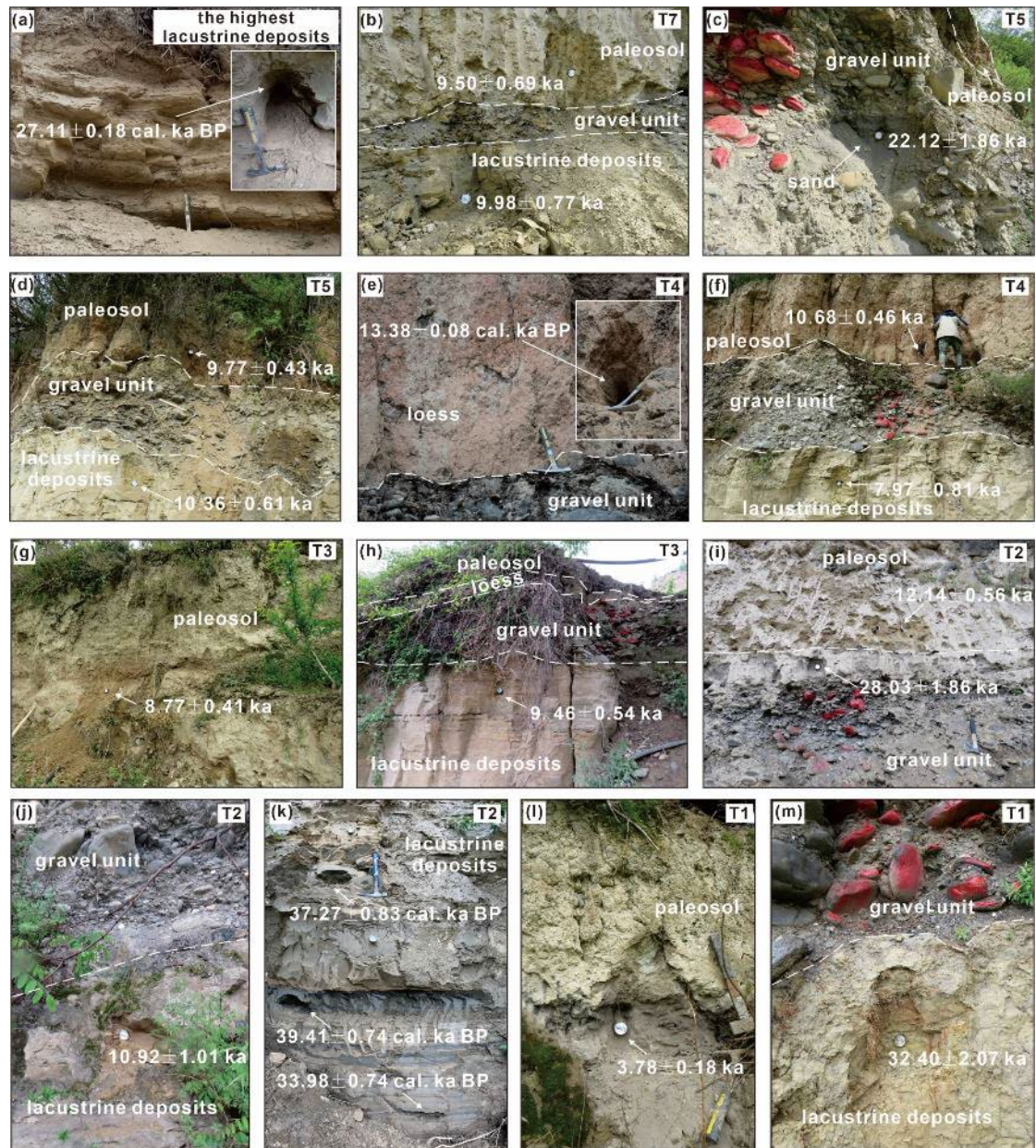


Figure 2. OSL and calibrated radiocarbon (denoted as cal. ka BP) dating results from Tuanjie. (a) The highest lacustrine deposits. (b) Lacustrine deposits and palaeosol at T7. (c) Gravel unit at T5. (d) Lacustrine deposits and palaeosol at T5. (e) Loess at T4. (f) Lacustrine deposits and palaeosol at T4. (g) Palaeosol at T3. (h) Lacustrine deposits at T3. (i) Gravel unit and palaeosol at T2. (j) Lacustrine deposits at T2. (k) Lacustrine deposits at T2. (l) Palaeosol at T1. (m) Lacustrine deposits at T1. White dashed lines mark unit boundaries.

185

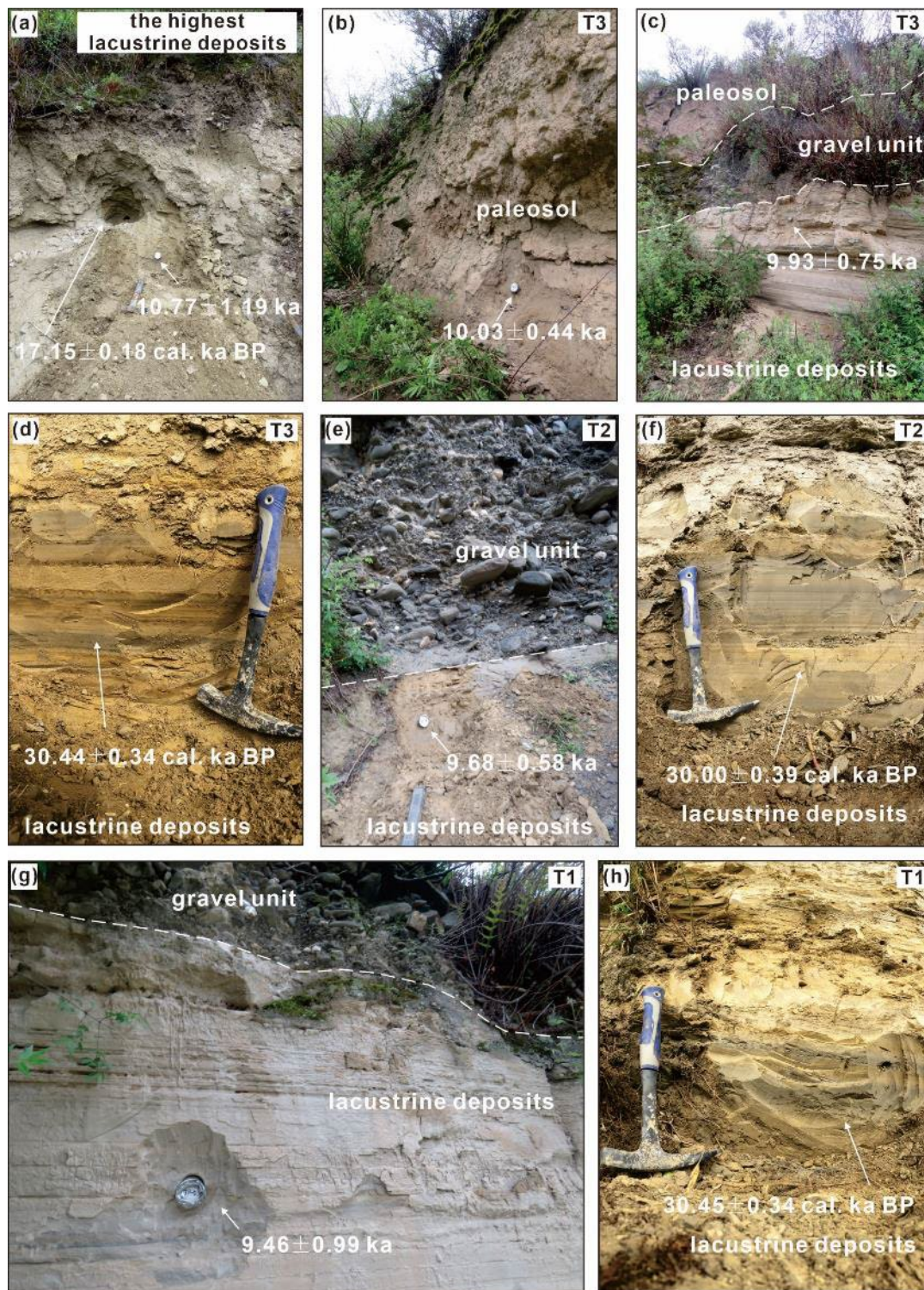


Figure 3. OSL and calibrated radiocarbon (denoted as cal. ka BP) dating results from Taiping. (a) Paired OSL and radiocarbon samples collected from the highest lacustrine deposits. (b) Palaeosol at T3. (c) Lacustrine deposits in T3. (d) Lacustrine deposits in T3. (e) Lacustrine deposits at T2. (f) Lacustrine deposits at T2. (g) Lacustrine deposits at T1. (h) Lacustrine deposits at T1. White dashed lines mark unit boundaries.

190

4 Results

195 4.1 Terrace geometry and distribution

The seven terraces at Tuanjie and three terraces at Taiping Terraces are all developed on thick lacustrine deposits (Fig. 4), which are naturally highly erodible. At Tuanjie, the lacustrine deposits are >200 m thick, and the longitudinal (stream-wise) lengths of the seven terraces range from 150 to 1000 m (Fig. 4, Table 2). The Taiping terraces are developed on a hillside with a slope of 40–60°, and is therefore influenced by landslides and some human activity. The lateral extent of T1, T2, and T3 varies from 190 to 520 m (Table 2). Correlations between the terrace levels at the two sites are given in Table 2 and Fig. 4.

205 **Table 2.** Elevation and correlation of terraces at Tuanjie and Taiping. Diexi Lake currently stands at ~ 2150 masl.

Tuanjie terraces	Elevation (masl)	Width (m)	Taiping terraces	Elevation (masl)	Width (m)
Highest	2390	-	Highest	2390	-
T7	2323	226	T3	2320	190
T6	2298	-	T2	2311	380
T5	2276	378	T1	2279	520
T4	2248	186	-	-	-
T3	2215	150	-	-	-
T2	2204	360	-	-	-
T1	2178	11000	-	-	-

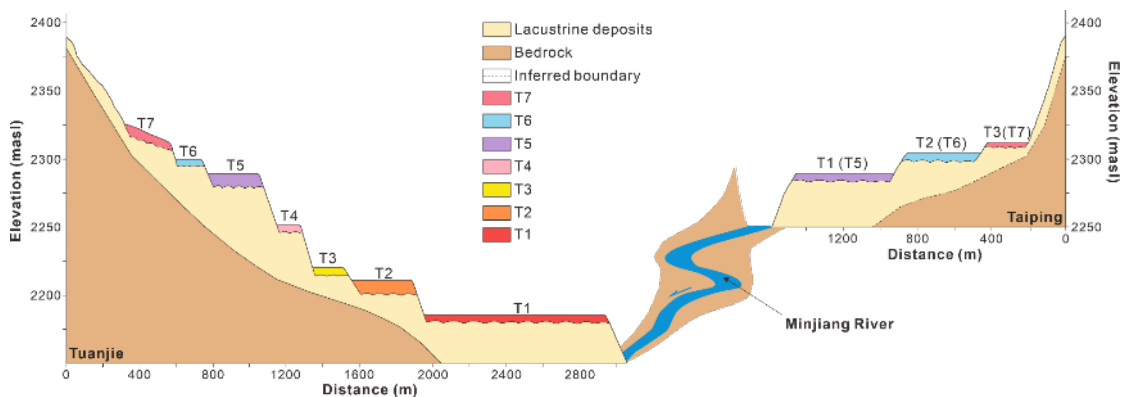


Figure 4. Sketch showing correlation between the Tuanjie and Taiping terraces (see Table 1).

210 4.2 Terrace lithostratigraphy

4.2.1 Tuanjie terraces

Tuanjie terraces T1, T2, T3, T4, and T6 are characterised by a sequence of silts, sands, gravels, loess, and palaeosol units. T5 and T7 lack the loess unit (Fig. 5a) probably due to erosion via human activities, and for the same reason T4, T5, T6 and T7 show strong signs of deformation and collapse. The lithostratigraphy (Table 1 and Fig. 5a) is summarised as follows (starting from the base):

(1) Silt clay (*Fl*), with intense weathering, horizontal bedding, and wave bedding, characteristic of lacustrine deposits.

(2) Gravelly (*Gh*, *Gci*, *Gmm*) fluvial deposits separated by an unconformity with the underlying lacustrine deposits. The flow orientation of the gravels is predominantly parallel to the Minjiang River, suggesting it is the source of these gravels. The gravel units at T1, T4, T5, and T7 (*Gh*) are generally poorly-sorted and well-rounded, with a grain-sizes ranging 2-30 cm. Present are longitudinal bedforms, lag deposits, and sieve deposits (Fig. 5a). At T2 (*Gci*) the gravels show inverse grading, with grain-sizes ranging 2-25 cm (clasts > 35 cm are rare), poorly-sorted and sub-circular to round clasts without orientation. At T3 (*Gci*), the gravel units exhibit inverse grading, are poorly sorted, with sub-circular to round clasts of grain-size ranging 3-25 cm. Gravels at T6 (*Gmm*) show graded bedding with good sorting and rounding.

(3) Loess (*Ls*), loess units of T1 and T2 are brick-red in colour; the loess at T3 contains angular fragments of phyllite.

(4) Palaeosols (*Ps*), if present, are developed capping the fluvial strata, and contain abundant roots (Fig. 5a). Lacustrine deposits extend above T7 with a thickness of 30 m; these deposits show undulating bedding and severe denudation (Fig. 4).

4.2.2 Taiping terraces

Taiping terraces are characterised by a sequence of lacustrine silts, muds, gravels, loess, and palaeosol units (Fig. 5b). The lithostratigraphy (Table 1 and Fig. 5b) is summarised as follows (starting from the base):

(1) Silt-clay (*Fl*) underlies all three terraces. Note that the highest extent of the lacustrine units reaches > 70 m thick.

(2) Gravelly (*Gh*, *Gci*, *Gmm*) fluvial deposits observed on the Taiping terraces all show a flow

direction aligned with Luobogou Gully, indicating these gravels derive from the gully. Gravels at T1
 240 (*Gcm*) are characterised by poorly sorted and subrounded gravels with grain-sizes of 5-10 cm. Similarly,
 the gravel units in T2 and T3 (*Gcm*) contain numerous broken phyllite fragments. T3 displays two beds
 of horizontal, angular phyllite fragments (*Gh*, *Gci*) with grain-sizes of 2-5 cm.

(3) Mud (*Fm*) units contain snail shells suggesting these may be overbank deposits, abandoned
 channels, or drape deposits.

245 (4) Loess (*Ls*) units at T2 and T3 are mixed with some angular phyllite fragments

(5) Palaeosols (*Ps*) cap all three terraces.

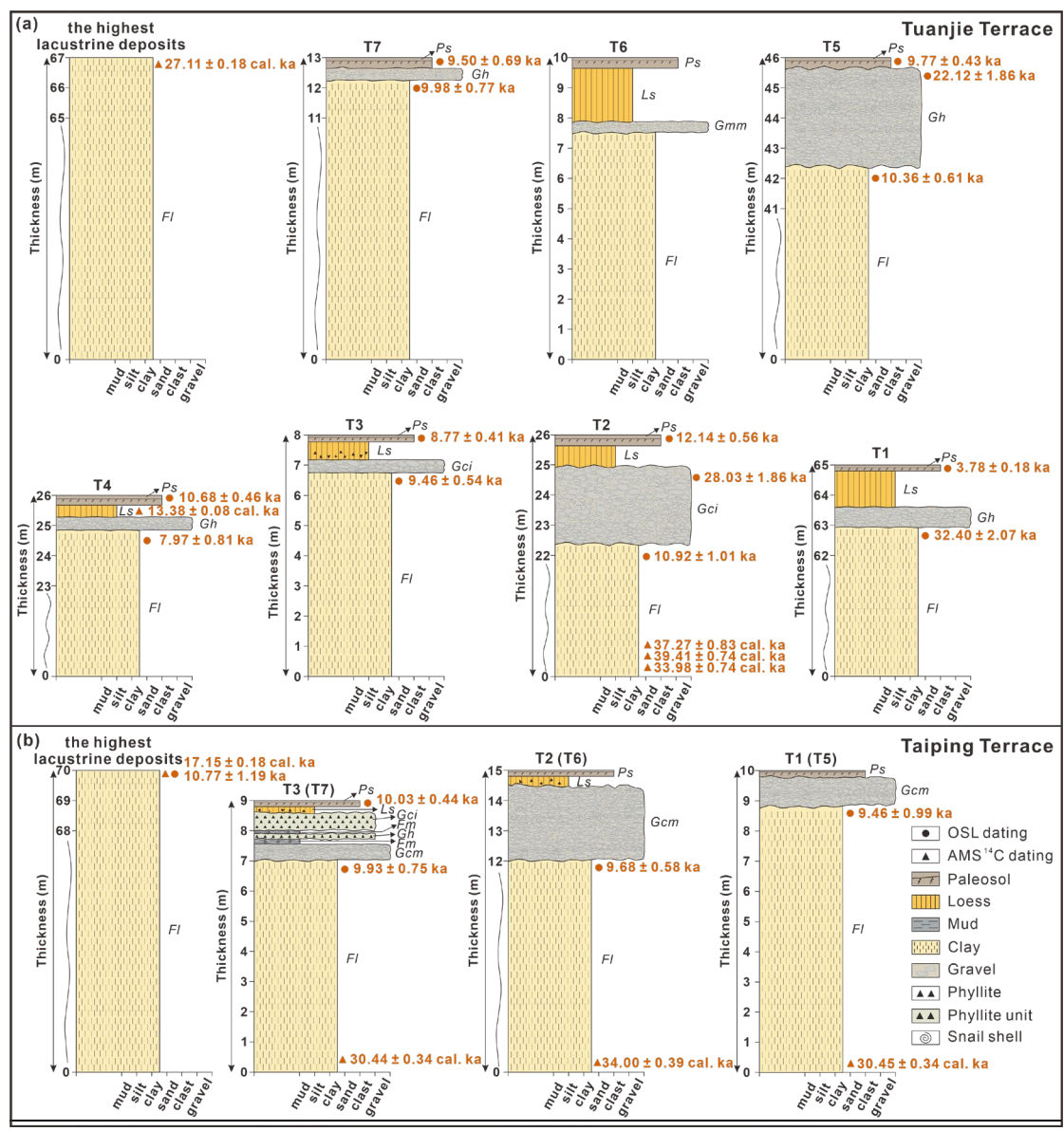


Figure 5. Terrace sedimentary sequences, lithofacies, and dating results (radiocarbon dates are denoted cal. ka): (a) Tuanjie T1, T2, T3, T4, T5, T6, T7, and the highest lacustrine deposits, respectively. (b)

250 Taiping T1, T2, T3, and the highest lacustrine deposits. All lithofacies labels are linked to Table 1; see
Table 2 and Fig. 4 for terrace correlations.

4.3 OSL ages

We measured 19 quartz OSL dates in total: 14 from Tuanjie and 5 from Taiping terraces (summarised
in Fig. 5 and Table 3).

255 At Tuanjie, the depositional ages of the lacustrine deposits range from ~32 ka to 10 ka and do not
follow a simple elevational sequence. T1, T2, T3, and T4 display a younging trend with increasing
elevation, while T5 and T7 yield similar ages, but are older than T3 and T4. Gravel units from T2 and T5
yield ages of 28 ± 2 ka and 22 ± 2 ka, respectively. The palaeosols are all Holocene in age, mostly ranging
from ~ 12 to 9 ka, with T1 yielding a notably younger age of ~ 4 ka.

260 At Taiping, the depositional ages of all three lacustrine samples (plus the highest lacustrine sample)
are consistently ~ 10 ka.

Table 3 Summary of OSL data.

Location	Terrace no.	Facies	Longitude and latitude	Quartz			Elevati on (masl)*	Sample depth (m)	U (ppm)	Th (ppm)	K (%)	Water content (%)	Dose rate (Gy/ka)	Dose (Gy)	Age (ka)
				Lab code	grain size (μm)	Sample ID									
Taiping	-	lacustrine	32°7'37"N, 103°44'14"E	IEE5554	4-11	TP19-1	2343	1.90	4.82±0.14	12.85±0.37	1.98±0.03	20±5	4.27±0.14	45.93±4.84	10.77±1.19
	T3	palaeosol	32°7'34"N, 103°44'12"E	IEE5555	4-11	TP19-2	2279	3.50	2.92±0.05	14.75±0.20	2.01±0.02	10±5	4.28±0.15	42.95±1.10	10.03±0.44
		lacustrine		IEE5556	4-11	TP19-3		4.20	3.62±0.55	14.23±0.27	2.20±0.04	20±5	4.17±0.16	41.43±2.68	9.93±0.75
		lacustrine	32°7'32"N, 103°44'11"E	IEE5557	4-11	TP19-4	2220	3.60	3.29±0.10	12.59±0.40	1.90±0.01	20±5	3.71±0.12	35.89±1.80	9.68±0.58
	T1	lacustrine	32°7'33"N, 103°44'11"E	IEE5558	4-11	TP19-5	2177	1.00	3.31±0.07	12.74±0.19	2.17±0.02	20±5	4.02±0.13	38.05±3.78	9.46±0.99
Tuanjie	T7	palaeosol	32°2'42"N, 103°39'45"E	IEE5540	4-11	DX19-1	2315	2.30	3.48±0.04	13.86±0.28	2.16±0.07	10±5	4.54±0.17	43.16±2.71	9.50±0.69
		lacustrine		IEE5541	4-11	DX19-2		2.90	3.41±0.05	14.00±0.20	2.40±0.05	20±5	4.29±0.14	42.82±2.99	9.98±0.77
	T5	palaeosol	32°2'42"N, 103°39'48"E	IEE5543	4-11	DX19-4	2266	1.30	2.93±0.07	13.49±0.21	2.03±0.02	10±5	4.25±0.15	41.47±1.05	9.77±0.43
		fluvial	32°2'46"N, 103°39'55"E	IEE5542	90-150	DX19-3	2265	2.60	2.28±0.05	10.25±0.17	1.53±0.04	10±5	2.70±0.11	59.74±4.46	22.12±1.86
		lacustrine	32°2'42"N, 103°39'48"E	IEE5544	4-11	DX19-5	2266	2.80	3.14±0.05	13.34±0.13	2.16±0.05	20±5	3.96±0.13	41.03±1.98	10.36±0.61
T4	palaeosol	32°2'40"N, 103°39'56"E	IEE5545	4-11	DX19-6	2229	2.20	2.85±0.03	14.35±0.10	2.00±0.01	10±5	4.24±0.15	45.33±1.14	10.68±0.46	
	lacustrine		IEE5546	4-11	DX19-7		5.00	3.57±0.06	14.13±0.36	2.45±0.04	20±5	4.34±0.15	34.59±3.33	7.97±0.81	
T3	palaeosol	32°2'40"N, 103°39'55"E	IEE5547	4-11	DX19-8	2192	2.20	2.99±0.29	12.78±0.19	1.96±0.07	10±5	4.11±0.16	36.05±0.91	8.77±0.41	
	lacustrine		IEE5548	4-11	DX19-9		2.10	3.12±0.16	13.54±0.21	2.48±0.02	20±5	4.26±0.14	40.26±1.85	9.46±0.54	
T2	palaeosol	32°2'46"N, 103°39'60"E	IEE5549	4-11	DX19-10	2180	5.00	3.40±0.05	13.97±0.23	2.41±0.06	10±5	4.70±0.18	57.06±1.52	12.14±0.56	
	fluvial		IEE5550	90-150	DX19-11		5.50	3.37±0.04	14.74±0.12	1.78±0.04	10±5	3.38±0.13	94.60±5.09	28.03±1.86	
T1	lacustrine	32°2'42"N, 103°40'08"E	IEE5551	4-11	DX19-12	2194	4.50	3.35±0.04	13.76±0.16	2.26±0.07	20±5	4.10±0.14	44.79±3.84	10.92±1.01	
	palaeosol	32°2'41"N, 103°40'11"E	IEE5553	4-11	DX19-14	2149	0.60	2.38±0.07	8.69±0.29	1.52±0.07	10±5	3.20±0.13	12.09±0.30	3.78±0.18	
	lacustrine	32°2'43"N, 103°40'13"E	IEE5552	4-11	DX19-13	2151	2.50	2.89±0.03	11.81±0.10	2.16±0.05	20±5	3.77±0.13	122.24±6.67	32.40±2.07	

*Given that the terraces are not completely flat, elevation data vary slightly from that in Table 2.

4.4 Radiocarbon ages

Nine radiocarbon ages were measured in total, all from bulk sediment samples (Table 4). The highest lacustrine deposits at Tuanjie and Taiping yielded ages of ~ 27 cal. ka BP and ~ 17 cal. ka BP, respectively. The loess sample collected from Tuanjie T4 yielded an age of ~ 13 cal. ka BP. The bottom lacustrine deposits of T2 yielded ages of ~ 34 , ~ 39 , and ~ 37 cal. ka BP. The depositional ages of all three bottom lacustrine samples of Taiping T1, T2, T3 are ~ 30 , ~ 34 , and ~ 30 cal. ka BP, respectively.

Table 4 Summary of the radiocarbon results for Tuanjie and Taiping.

Samples	Lab code	Material	Elevation (masl)	$\delta^{13}\text{C}$ (‰)	Radiocarbon age (a BP)	Calibration age (cal. ka BP)
TP-max	Beta-520926	bulk sediment	2342.95	-19.1	14050 \pm 50	17.15 \pm 0.18
TP23-03	Beta-664881	bulk sediment	2311.00	-18.5	26040 \pm 120	30.44 \pm 0.34
TP23-02	Beta-664890	bulk sediment	2279.00	-19.9	29350 \pm 160	34.00 \pm 0.39
TP23-01	Beta-664882	bulk sediment	2269.00	-16.1	26010 \pm 120	30.45 \pm 0.34
TJ-max	Beta-520925	bulk sediment	2390.00	-19.2	22740 \pm 90	27.11 \pm 0.18
TJ-T4-HT	Beta-520924	bulk sediment	2280.00	-21.6	11490 \pm 40	13.38 \pm 0.08
TJ23-03	Beta-664879	bulk sediment	2179.50	-17.7	32670 \pm 240	37.27 \pm 0.83
TJ23-02	Beta-664878	bulk sediment	2178.60	-17.3	34170 \pm 280	39.41 \pm 0.74
TJ23-01	Beta-664877	bulk sediment	2178.00	-17.2	29300 \pm 170	33.98 \pm 0.74

5 Discussion

5.1 Reliability of dating results

First, we consider the reliability of our chronology. Given the relatively stable depositional environment of the silt-rich (lacustrine and palaeosol) samples and the normal distribution of D_e , we assume they were well-bleached before deposition and therefore yield reliable ages.

Our ages are consistent with those reported by previous studies at Diexi, which fall mainly between about 36 and 11 ka (Table S2). We note that the older ages of the Tuanjie and Taiping lacustrine deposits (Fig. 5a) are ~ 35 ka and ~ 30 ka, respectively; however, two other published sources support our result: (1) a basal radiocarbon age (calibrated to 35.1 ± 0.3 cal. ka BP) reported from the Diexi Lake ZK2 drill-core (Wang et al., 2012), and (2) two radiocarbon ages from another lacustrine section at Tuanjie (calibrated to 35.8 ± 0.4 , and 30.7 ± 0.03 cal. ka BP) reported by Zhang et al. (2009).

Both gravel units at Tuanjie T2 and T5 (~ 28 and 22 ka, respectively) yield OSL ages that are much older than the underlying lacustrine deposits (~ 11 and 10 ka, respectively) (Fig. 5). In this case, we favour the lacustrine ages and exclude the samples collected from thin sand lenses within the gravels.

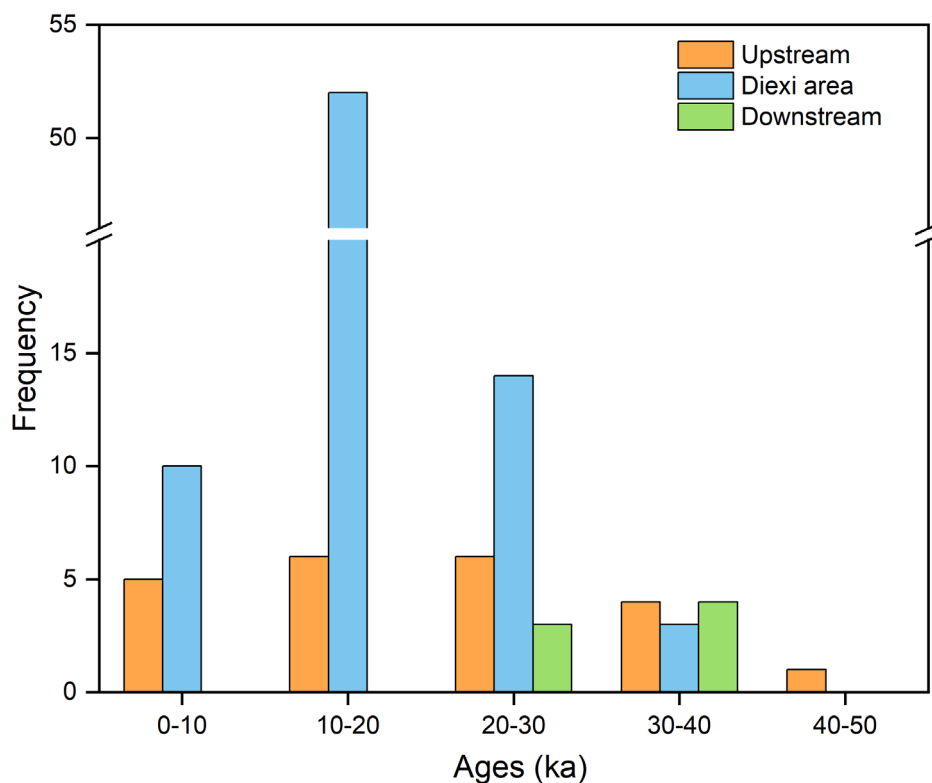
305 At Taiping, our radiocarbon-OSL dating pair collected from the highest lacustrine deposits yields ages of 17.2 ± 0.2 cal. ka BP and 10.8 ± 1.2 ka, respectively (Fig. 5). In this case, we suspect the radiocarbon age is overestimated due to the ‘old carbon reservoir’ effect. This reservoir effect in the sample can result from several factors, including: (1) the lower ^{14}C -activity carbon and the atmosphere-water exchange (Deevey et al., 1954; Keaveney and Reimer, 2012; Ascough et al., 2016); (2) landslides, debris flows, or other disturbances causing surface sediments to drop into the lake, mixing older
310 sediments with new (Counts et al., 2015; Shi, 2020); and (3) the re-deposition of older organic components, such as stored charcoal (Kaplan et al., 2002; Krivonogov et al., 2016).

5.2 Terraces along the upper Minjiang River

A minimum of fifteen sets of river terraces occur along the upper Minjiang River valley, with nine
315 sets located upstream of Diexi (from Gonggaling to Zhangla), two sets near Diexi (Taiping and Tuanjie), and four sets downstream (the Maoxian-Wenchuan area). From previously published work, we compiled a total of 124 dates (OSL, infra-red stimulated luminescence, thermoluminescence, radiocarbon and Electron spin resonance) measured on the terraces of the upper Minjiang River (Table S2). Terraces upstream of Diexi go as far back as ~ 830 ka (Zhao et al., 1994), but fall primarily between ~ 47 and 2
320 ka (Fig. 6). Terraces in the Diexi area span ~ 505 to 2 ka (Kirby et al., 2000; Duan et al., 2002; Yang et al., 2003; Gao and Li, 2006; Wang et al., 2007; Wang, 2009; Mao, 2011; Jiang et al., 2014; Zhong, 2017; Guo, 2018; Luo et al., 2019; Zhang, 2019; Wang et al., 2020b) with the majority, 32-2 ka (Fig. 6). Downstream reaches host terraces ranging ~ 400 to 50 ka (Zhao et al., 1994; Yang et al., 2003; Yang, 2005; Zhu, 2014), with a significant fraction falling between ~ 40 and 20 ka (Fig. 6).

325 Terraces upstream (Zhangla basin to the source of the Minjiang) are attributed to tectonic uplift (Yang et al., 2003; Yang, 2005; Yang et al., 2008; 2011; Chen and Li, 2014; Zhu, 2014). Whereas, by contrast, the Tuanjie and Taiping terraces are thought to relate to the evolution of the Diexi palaeo-dam (Duan et al., 2002; Wang et al., 2005a; Wang, 2009; Zhu, 2014). Terraces downstream in the Maoxian-Wenchuan region share similar characteristics to those at Diexi, as they are also believed to have formed
330 via outburst flooding from a palaeo-dammed lake (Zhu, 2014). However, those terraces are also strongly

influenced by activity along the Maoxian-Wenchuan fault zone. We hypothesise that the formation and evolution of the Diexi terraces (at Tuanjie and Taiping) are distinct and independent of the upstream and downstream terraces. We test and discuss this idea further in the following sections.



335 **Figure 6.** Frequency distribution histogram of terrace ages since 50 ka in the upper reaches of the Minjiang River (at Diexi, upstream, and downstream). By far the most frequent terrace age falls between 20 and 10 ka.

5.3 Correlation of the Tuanjie and Taiping terraces

The highest lacustrine deposits at Tuanjie and Taiping occur at the same elevation (~ 2390 masl), suggesting that the two sets of terraces are also related somehow. The Tuanjie and Taiping terraces certainly share similar lithostratigraphy (Fig. 5). For instance, Tuanjie T5/Taiping T1 share the same sedimentary sequence (from the base to top): silty-clays (*Fl*), gravels (*Gh* at Tuanjie, *Gcm* at Taiping) and palaeosol (*Ps*), and very similar sequences are shared by Tuanjie T6/Taiping T2, and Tuanjie T7/Taiping T3. In addition, the chronology (Table 3) we have from the lacustrine deposits at Taiping T1 (9.5 \pm 1 ka) and Tuanjie T5 (10.4 \pm 0.6 ka) compare closely, as do Taiping T3 (10 \pm 0.8 ka) and Tuanjie T7 (10 \pm 0.8 ka). Based on these considerations, together with their elevation, we suggest that Taiping T1, T2, and T3 correspond to Tuanjie T5, T6 and T7 (Fig. 4).

5.4 Controls on terrace formation at Diexi: tectonism, climate or outburst floods?

The formation of terraces in mountain rivers is typically attributed to either tectonic activities
350 (Burgette et al., 2017), climate change (Maddy et al., 2005; Gao et al., 2020), or some combination of
those (Luo et al., 2019; Chen et al., 2020; Narzary et al., 2022; Ma et al., 2023). The impact of extreme
events on terraces has come to the attention of researchers more recently (Hewitt, 2016; Wang et al.,
2021; Yu et al., 2021). At Diexi, the great thickness (> 200 m) of lacustrine deposits carved by floodwaters
and topped discontinuously by terrace gravels and loess-palaeosol sequences, suggests a role for
355 tectonism, climate, and outburst floods, but the relative influence of each is yet to be clarified. We pursue
this question below.

5.4.1 Effects of tectonism on the Diexi terraces

The Tuanjie and Taping terrace sites are sufficiently close (12 km) to be considered subject to the
equivalent tectonic forcing. In Section 5.2, we divided the upper Minjiang River into three segments:
360 Gonggaling to Zhangla (upstream of Diexi), the Diexi area, and the Maoxian-Wenchuan area
(downstream of Diexi). Since the initial damming at the Diexi palaeo-landslide, the fluvial incision rates
in these three segments of the upper Minjiang is measured at 8.3–85.3 mm/yr, 13.6–198 mm/yr, and 58
mm/yr, respectively (see Table S2). In comparison, the Minshan Block (which includes the reach from
Gonggaling to Maoxian) is thought to have experienced an average uplift rate of 1.5 mm/yr during the
365 Quaternary (Zhou et al., 2000). Clearly, recent incision rates in the Diexi area have been several-times
faster than the average uplift rate of the Minshan Block. This highlights the unique character of Diexi
and suggests that tectonic activity is not a primary factor in the formation of the terraces.

5.4.2 Effects of climate changes on the Diexi terraces

The regional climate has undergone three transitions from cold-dry to warm-humid climate between
370 ~ 40 and 30 ka (Zhang et al., 2009) followed by more than ten alternations of cold to warm between 30
and 10 ka (Wang, 2009; Wang et al., 2014). The terraces at Tuanjie and Taiping span the past 39 ka, so
to investigate the influence of climate we examine the climate variations over the same period (Fig. 7).
The four climate proxies reveal significant fluctuations from the end of the Last Glacial Maximum (LGM)
to the early Holocene followed by relative stability throughout the Holocene.

375 It is tempting to speculate that warmer periods triggered wetter conditions or glacier melt leading

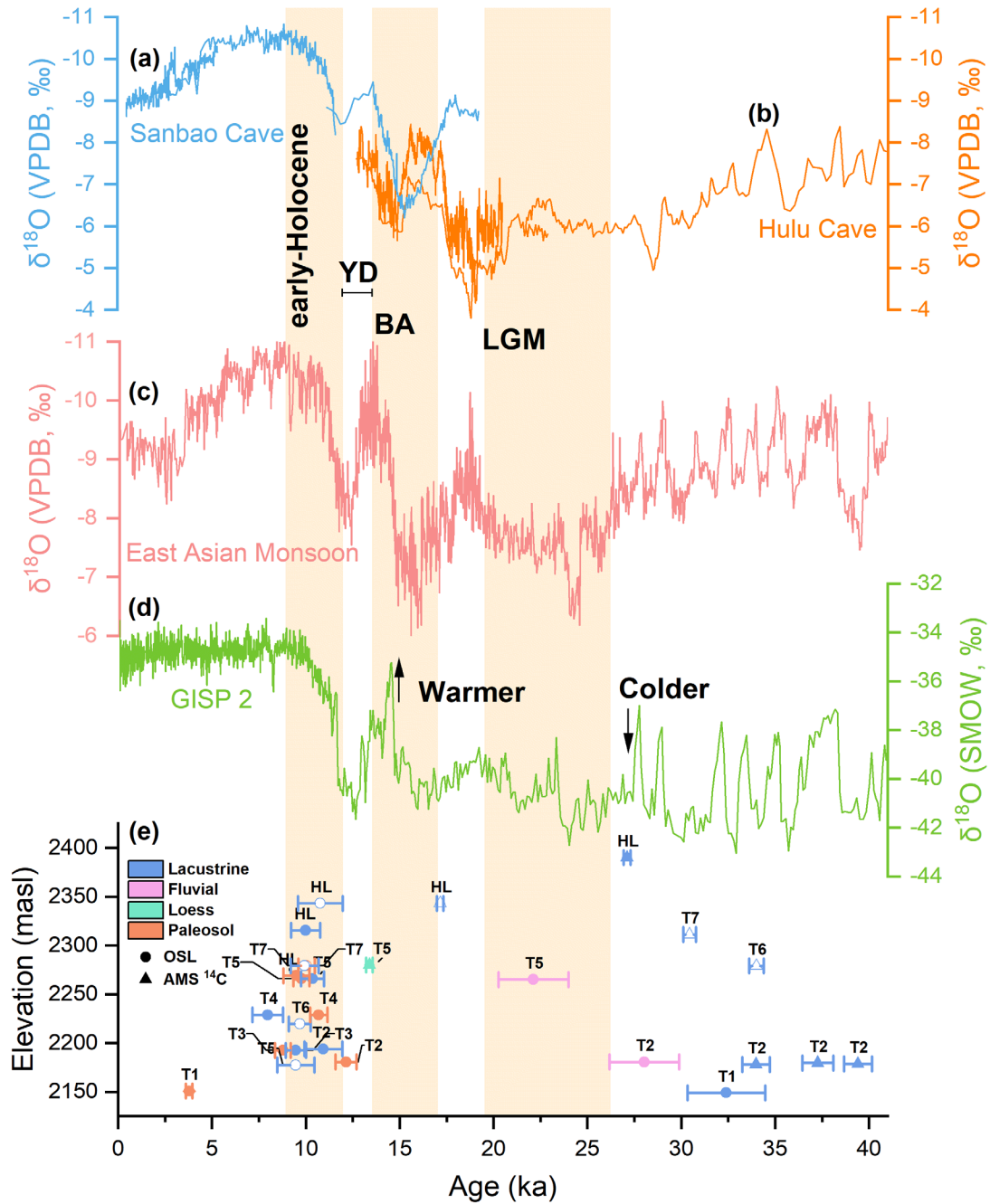
to the overtopping of the palaeo-dam and formation of terraces; however, we cannot see any clear relationship between the age of the terraces and the climatic variations over the past 39,000 yrs (Fig. 7). Nevertheless, two important points are worth making:

(1) A fluctuating climate may be seen in terrace geometry. In papers by Mao (2011), Jiang et al. (2014), and Shi (2020), it is argued that Tuanjie T2 displays an irregular sequence of ages with depth that suggest repeated fluctuations in the lake level by up to 11 m between 19 and 11 ka (the deglaciation period) (Table S2). Regarding Tuanjie T1, we note the extraordinary terrace width. There are three possible factors that created the very wide T1 terrace: (i) During this period, strong monsoon activity resulted in high discharges and low sediment input, leading to river incision (Malatesta and Avouac, 2018; Tian et al., 2021; Yu et al., 2021). (ii) We note some additional erosion may have occurred owing to the positioning of the Tuanjie terraces on the concave margin of the valley (Fig. 1b) where lateral fluvial erosion tends to be accentuated. (iii) As the lowest terrace, Tuanjie T1 was subjected to frequent erosion during the progressive outburst of the palaeo-dam (Phase IV to Phase VII, Fig. 9).

(2) Some degree of climate control can be recognised in terms of the aeolian and weathering processes. The loess unit at Tuanjie T4 ($\sim 13.4 \pm 0.1$ cal. ka BP) dates to just before the Younger Dryas reflecting a cool depositional environment; loess observed at Tuanjie T3 and T2, as well as Taiping T3 and T2 suggest ages slightly younger. Most of the palaeosol units relate to the warming conditions of the early Holocene.

(3) The three outburst floods (~ 27 ka, ~ 17 ka and ~ 12 ka, reported in Section 5.5) in Diexi area were happened at the climate fluctuation periods. We speculated these floods may be the result of the glacial melting. As Wang et al. (2012) mentioned that during the Last Glacial Period, the melting of glaciers triggered massive hillslopes instability, and formed palaeo-dammed lakes.

(4) The absent of outburst flood in the Holocene may be related to the warm and stable climate.



400

Figure 7. Palaeoclimate ($\delta^{18}\text{O}$) proxies compared with the OSL and radiocarbon chronologies obtained from the Diexi terraces. (a) Sanbao Cave (Wang et al., 2008); (b) Hulu Cave (Wang et al., 2001); (c) East Asian Monsoon (Cheng et al., 2016); (d) GISP-2 (Grootes et al., 1993); and (e) the Diexi terraces at Tuanjie (solid symbol) and Taiping (hollow symbol). The early Holocene, Younger Dryas (YD), Bølling-Allerød interstadial (BA), and the Last Glacial Maximum (LGM) are labelled.

405

5.5 Terrace formation and the evolution of the Diexi palaeo-landslide dam

Damming and outburst floods can strongly impact upstream and downstream areas, causing

aggradation and incision (Fig. 8) (Hewitt et al., 2008; Korup and Montgomery, 2008). A lake formed by the blockage of a river can raise water levels upstream, resulting in the potential upstream flooding (Guo et al., 2016), and following an outburst flood, the lake level drops as a result of sudden erosion at the crest of the dam. During this lower lake level, the river cuts through the easily eroded lacustrine deposits, forming terraces.

The triangle formed by Tuanjie, Jiaochang and Xiaohaizi (Fig. 1b) marks the centre of the palaeo-dammed Diexi Lake. We suggest that this ancient lake has experienced multiple damming and breach events leading to major outburst floods down the Minjiang River. For instance, high magnitude outburst sediments are identified downstream around the Xiaoguanzi-Manaoding (Fig. 1b). Based on our terrace lithofacies and chronological analyses, we attempt to reconstruct the history of river blocking and outburst floods sourced from the Diexi Lake, as follows.

The Minjiang River was blocked by the Diexi palaeo-landslide sometime before 35 ka (Phase I: > 35 ka), as indicated by five lines of evidence: (1) the bottom lacustrine deposits of Tuanjie T2 dated to ~ 35 ka; (2) the deposition age of Taiping T2 was ~ 34 ka; (3) the basal radiocarbon age in a drill-core from Diexi Lake is 35.1 ± 0.3 cal. ka BP (Wang et al., 2012) (note the lacustrine pile extends ~ 80 m deeper); (4) at Xiaoguanzi, lacustrine sediments dated to 34.9 ± 0.8 and 35.6 ± 0.8 cal. ka BP (Wang et al., 2012) are observed capping part of the palaeo-landslide dam; and (5) the same occurs at Manaoding dated to 34.5 ± 0.2 cal. ka BP (Wang et al., 2012).

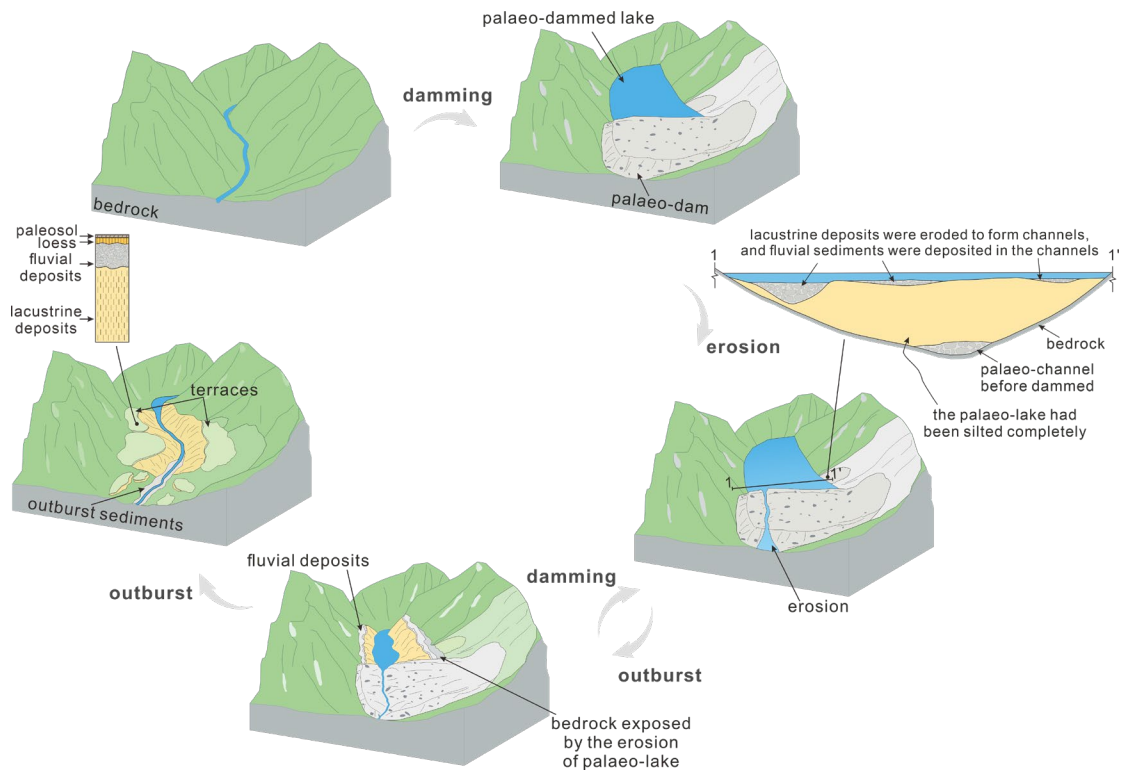
After being initially blocked by the palaeo-landslide, Diexi Lake reached its highest level around 27 ka (highest lacustrine sediments at Tuanjie date to 27.1 ± 0.2 ka, Fig. 5a). This matches the timing of evidence of the first known outburst flood (Phase II: ~ 27 ka), a gravelly unit near Xiaoguanzi (Fig. 1b), OSL-dated by Ma et al. (2018) at 27.3 ± 2.8 ka. Further evidence of an outburst flood (or floods) around 27 ka is indicated by two other nearby sites dated with OSL and radiocarbon, respectively: (1) a 35 m-thick sequence of deformed lacustrine bedding at Shawan (Wang et al., 2011; Wang et al., 2012), and (2) convolution structures exposed near Jiaochang (Fig. 1b) (Wang et al., 2012). Around ~ 27 ka appears to have been a time of major perturbation in the upper Minjiang River: a palaeo-landslide at Qiangyang (Fig. 1b) is radiocarbon-dated to 26.5 ± 0.5 ka, 27.3 ± 0.4 cal. ka BP (Wang et al., 2012); and downstream, a palaeo-dammed lake at Maoxian is radiocarbon-dated to 26.8 ± 1.0 cal. ka BP (Wang et al., 2007).

The Diexi palaeo-dam was re-established and sedimentation in the lake resumed for about 10,000 yrs (Phase III: ~ 27–17 ka), as indicated by the highest lacustrine sediments at Taiping dated to $17.2 \pm$

0.2 cal. ka BP (Fig. 5b).

The second outburst flood (or floods) occurred ~ 17 ka (Phase IV). This event incised the palaeo-dam, causing the Diexi Lake level to drop by ~ 110 m (to 2279 masl), as recorded at Taiping T1 and Tuanjie T5 (Fig. 5a, b). The lowering of the lake level exposed the highest lacustrine deposits at Taiping. The palaeo-landslide at Manaoding, dated to 16.8 ± 0.6 cal. ka BP (Wang et al., 2012), is possibly linked to this second outburst flood.

In the 5000 yrs that followed (Phase V: ~ 17–12 ka), two more outburst floods may have lowered the palaeo-dam further (forming Tuanjie T4 and T3), although the timing is uncertain. Yet, we can say with confidence that an outburst flood ~ 12 ka (Phase VI), lowered the palaeo-dam by ~ 70 m (to 2204 masl), forming Tuanjie T2. From ~ 12 ka to the present (Phase VII), it appears the Diexi palaeo-dam crest has gradually incised to its current level ~ 2150 masl (aside from the brief period at a higher level following the 1933 Diexi earthquake, Dai et al., 2021).

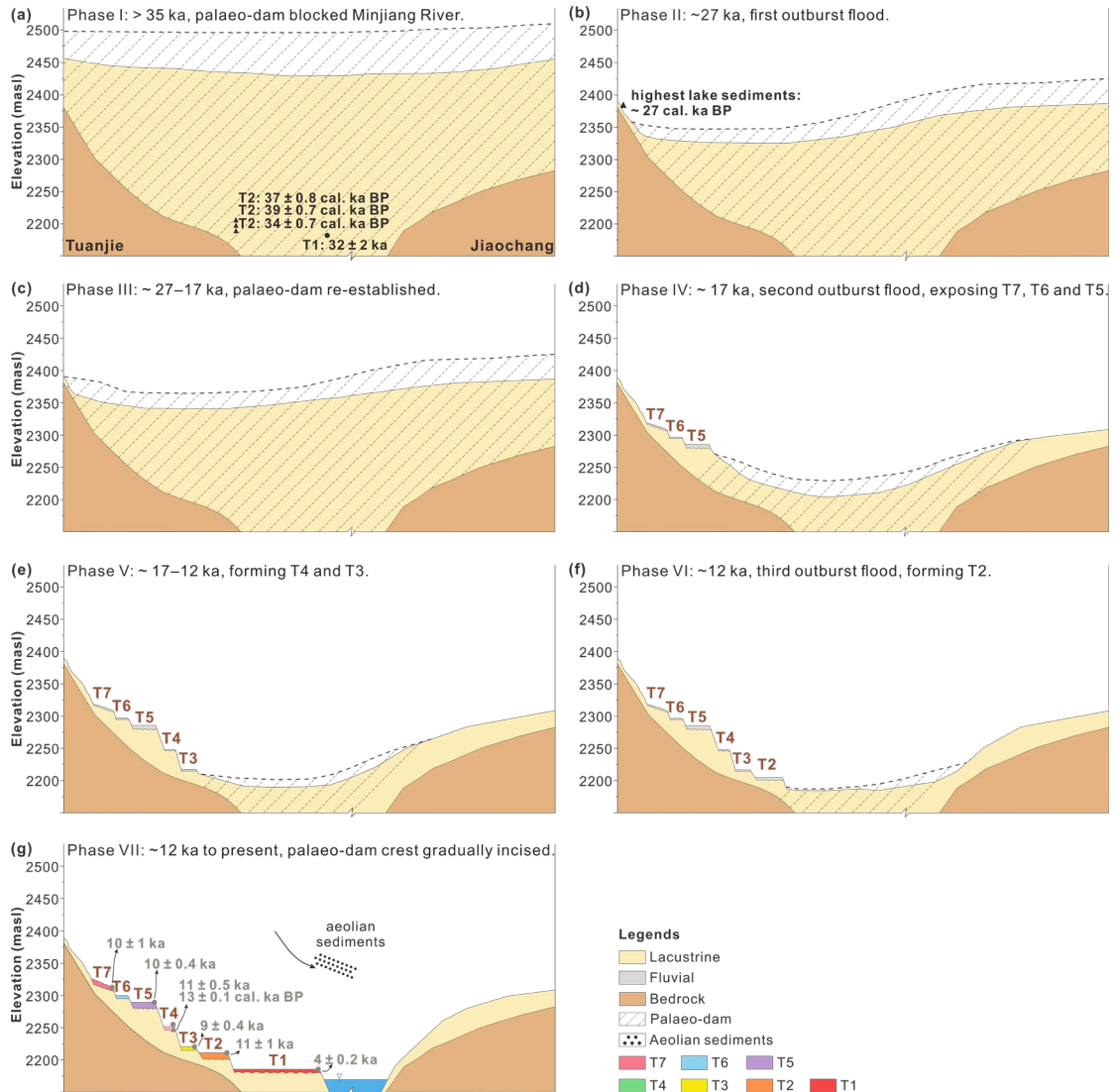


450

Figure 8. Model of palaeo-landslide dam evolution through time, starting with a blocking event (e.g., a major landslide), which then becomes a natural dam on the river causing a lake to form. Lacustrine deposits accumulate behind the dam, sometimes to great depth (at Diexi lacustrine sediments are > 200 m-thick). A positive water balance in the lake triggers overtopping of the dam, causing potentially catastrophic outburst floods downstream. The outburst flood typically erodes the crest of the dam

455

subsequently lowering the lake level and allowing fluvial processes to resume along parts of the valley. This repeated process yields a terrace stratigraphy comprising (from base to top): lacustrine deposits topped by fluvial deposits perhaps capped by loess and palaeosol development.



460 **Figure 9.** Schematic model of the evolution of the Diexi palaeo-dam and Tuanjie terraces. See Section
5.5 for detailed descriptions of each phase. Brown text denotes the ages of loess and palaeosol units.

6 Conclusions

We set out to investigate the origin and chronology of two sets of outstanding terraces formed upstream of the giant river-blocking Diexi palaeo-landslide on the upper Minjiang River, eastern Tibetan Plateau.

The Tuanjie terraces have seven levels (T1-T7), while those at Taiping have three (T1-T3). All

terraces display a consistent sedimentary sequence comprising thick lacustrine muds topped by fluvial gravels, which at a few sites are capped by loess and a palaeosol. We correlate T5, T6 and T7 at Tuanjie with T1, T2 and T3 at Taiping.

470 Our reconstruction of the history of terrace formation suggests two damming and three outburst events have occurred at the Diexi palaeo-landslide over the past 35,000 years. The sequence of events is summarised as follows: a giant landslide (>300 m high) blocked the river before 35 ka followed by the first outburst flood at ~ 27 ka; the river was blocked again between 27 to 17 ka followed by a second outburst at ~17 ka; and a third outburst at ~12 ka was followed by gradual fluvial incision of the palaeo-
475 dam crest to its current level.

Our findings at Diexi provide a detailed case study of terrace formation linked to the evolution of the palaeo-landslide dam. The Diexi terraces (at Tuanjie and Taiping) are distinct and independent of the upstream and downstream terraces along the upper Minjiang River—they are not directly the product of either tectonic or climate forcing. Instead, terrace height and geometry are the result of the sequence of
480 outburst floods that progressively lowered the crest of the palaeo-landslide dam (the local base level to the terraces) since its emplacement more than 35,000 years ago.

This study proposes a new perspective on terrace formation in steep rivers draining landslide-dominated mountain belts. Given the frequent observation of valley blocking dams in high mountain settings, we suspect that the terrace formation processes described here may be more widespread than
485 has been previously recognised.

Author contributions

JL wrote the manuscript and analysed the data; JDJ reframed data interpretations and revised the text comprehensively following review; XF and ZD discussed the results and provided guidance and funding; SK conducted the OSL dating; and ML polished the language.

490 Competing interests

An author is a member of the editorial board of the journal, *Earth Surface Dynamics*. The peer-review process was guided by an independent editor, and the authors have no other competing interest to declare.

Acknowledgments

495 We thank Lanxin Dai, Chengbin Zou, Yujin Zhong, Binbin Luo, Bing Xia, Kunyong Xiong, Wei He
for fieldwork assistance, and Xiangyang Dou for revising the figures.

Financial support

This research is financially supported by the Funds for National Science Foundation for Outstanding
Young Scholars, Grant no. 42125702, the National Natural Science Foundation of China, Grant no.
500 42207223, the Natural Science Foundation of Sichuan Province, Grant no. 2022NSFSC003, and the State
Key Laboratory of Geohazard Prevention and Geoenvironment Protection Independent Research Project,
Grant no. SKLGP2021Z025.

References

- An, W., Zhao, J., Yan, X., Li, Z., and Su, Z.: Tectonic deformation of lacustrine sediments in qiangyang
505 on the Minjiang fault zone and ancient earthquake, *Seismology and Geology*, 30, 980-988,
<https://doi.org/10.3969/j.issn.0253-4967.2008.04.014>, 2008.
- Arzhannikov, S., Arzhannikova, A., Ivanov, A., Demonterova, E., Yakhnenko, A., Gorovoy, V., and
Jansen, J.: Lake Baikal highstand during MIS 3 recorded by palaeo-shorelines on Bolshoi Ushkanii
Island, *Boreas*, 50, 101-113, <https://doi.org/10.1111/bor.12464>, 2020.
- 510 Arzhannikov, S. G., Ivanov, A. V., Arzhannikova, A. V., Demonterova, E. I., Jansen, J. D., Preusser, F.,
Kamenetsky, V. S., and Kamenetsky, M. B.: Catastrophic events in the Quaternary outflow history
of Lake Baikal, *Earth-Science Reviews*, 177, 76-113,
<https://doi.org/10.1016/j.earscirev.2017.11.011>, 2018.
- Ascough, P. L., Cook, G. T., Church, M. J., Dunbar, E., Einarsson, Á., McGovern, T. H., Dugmore, A. J.,
515 Perdikaris, S., Hastie, H., Friðriksson, A., and Gestsdóttir, H.: Temporal and Spatial Variations in
Freshwater¹⁴C Reservoir Effects: Lake Mývatn, Northern Iceland, *Radiocarbon*, 52, 1098-1112,
<https://doi.org/10.1017/s003382220004618x>, 2016.
- Avsin, N., Vandenbergh, J., van Balen, R., Kiyak, N. G., and Ozturk, T.: Tectonic and climatic controls
on Quaternary fluvial processes and river terrace formation in a Mediterranean setting, the Goksu
520 River, southern Turkey, *Quaternary Research*, 91, 533-547, <https://doi.org/10.1017/qua.2018.129>,
2019.
- Bell, C. M.: Punctuated drainage of an ice-dammed quaternary lake in southern South America, *Geogr
Ann A*, 90a, 1-17, <https://doi.org/10.1111/j.1468-0459.2008.00330.x>, 2008.
- Caputo, R., Salviulo, L., and Bianca, M.: Late Quaternary activity of the Scorciabuoi Fault (southern
525 Italy) as inferred from morphotectonic investigations and numerical modeling, *Tectonics*, 27, 1-18,
<https://doi.org/10.1029/2007tc002203>, 2008.
- Chen, G., Zheng, W., Xiong, J., Zhang, P., Li, Z., Yu, J., Li, X., Wang, Y., and Zhang, Y.: Late Quaternary
fluvial landform evolution and controlling factors along the Yulin River on the Northern Tibetan

- Plateau, *Geomorphology*, 363, <https://doi.org/10.1016/j.geomorph.2020.107213>, 2020.
- 530 Chen, H. and Li, Y.: River terrace responding to the obduction of the Longmenshan fault zone in the upper Min River basin, *Mountain Research*, 32, 535-540, <https://doi.org/10.16089/j.cnki.1008-2786.2014.05.003>, 2014.
- Chen, Y., Aitchison, J. C., Zong, Y., and Li, S.-H.: OSL dating of past lake levels for a large dammed lake in southern Tibet and determination of possible controls on lake evolution, *Earth Surface Processes and Landforms*, 41, 1467-1476, <https://10.1002/esp.3907>, 2016.
- 535 Chen, Z. and Lin, Q.: Significance of neotectonic movement of lake extension and shrinkage in Qinghai-Tibet Plateau, *Earthquake*, 31-40+52, <https://doi.org/CNKI:SUN:DIZN.0.1993-01-006>, 1993.
- Cheng, H., Edwards, R. L., Sinha, A., Spötl, C., Yi, L., Chen, S., Kelly, M., Kathayat, G., Wang, X., Li, X., Wang, X., Wang, Y., Ning, Y., and Zhang, H.: The Asian monsoon over the past 640,000 years and ice age terminations, *Nature*, 534, 640-646, <https://doi.org/10.1038/nature18591>, 2016.
- 540 Counts, R. C., Murari, M. K., Owen, L. A., Mahan, S. A., and Greenan, M.: Late Quaternary chronostratigraphic framework of terraces and alluvium along the lower Ohio River, southwestern Indiana and western Kentucky, USA, *Quaternary Science Reviews*, 110, 72-91, <https://doi.org/10.1016/j.quascirev.2014.11.011>, 2015.
- 545 Dai, L., Fan, X., Jansen, J. D., and Xu, Q.: Landslides and fluvial response to landsliding induced by the 1933 Diexi earthquake, Minjiang River, eastern Tibetan Plateau, *Landslides*, 18, 3011-3025, <https://doi.org/10.1007/s10346-021-01717-2>, 2021.
- Dai, L., Fan, X., Wang, D., Zhang, F., Yunus, A. P., Subramanian, S. S., Rogers, J. D., and Havenith, H.-B.: Electrical resistivity tomography revealing possible breaching mechanism of a Late Pleistocene long-lasting gigantic rockslide dam in Diexi, China, *Landslides*, 20, 1449-1463, <https://10.1007/s10346-023-02048-0>, 2023.
- 550 Deevey, E. S., Gross, M. S., Hutchinson, G. E., and Kraybill, H. L.: The natural ¹⁴C contents of materials from hard-water lakes, *Proceedings of the National Academy of Sciences*, 40, 285-288, <https://doi.org/10.2307/88928>, 1954.
- 555 Deng, B., Liu, S., Liu, S., Jansa, L., Li, Z., and Zhong, Y.: Progressive Indosinian N-S deformation of the Jiaochang structure in the Songpan-Ganzi fold-belt, Western China, *PLoS One*, 8, e76732, <https://doi.org/10.1371/journal.pone.0076732>, 2013.
- do Prado, A. H., de Almeida, R. P., Galeazzi, C. P., Sacek, V., and Schlunegger, F.: Climate changes and the formation of fluvial terraces in central Amazonia inferred from landscape evolution modeling, *Earth Surf Dynam*, 10, 457-471, <https://doi.org/10.5194/esurf-10-457-2022>, 2022.
- 560 Duan, L., Wang, L., Yang, L., and Dong, X.: The ancient climatic evolution characteristic reflected by carbon and oxygen isotopes of carbonate in the ancient barrier lacustrine deposits, Diexi, Minjiang River, *The Chinese Journal of Geological Hazard and Control*, 13, 91-96, <https://doi.org/10.3969/j.issn.1003-8035.2002.02.019>, 2002.
- 565 Duller, G. A. T.: Distinguishing quartz and feldspar in single grain luminescence measurements, *Radiation Measurements*, 37, 161-165, [https://10.1016/s1350-4487\(02\)00170-1](https://10.1016/s1350-4487(02)00170-1), 2003.
- Durcan, J. A., King, G. E., and Duller, G. A. T.: DRAC: Dose Rate and Age Calculator for trapped charge dating, *Quaternary Geochronology*, 28, 54-61, <https://10.1016/j.quageo.2015.03.012>, 2015.
- Fan, X., Dai, L., Zhong, Y., Li, J., and Wang, L.: Recent research on the Diexi paleo-landslide: dam and lacustrine deposits upstream of the Minjiang River, Sichuan, China, *Earth Science Frontiers*, 28, 71-84, <https://doi.org/10.13745/j.esf.sf.2020.9.2>, 2021.
- 570 Fan, X., Xu, Q., van Westen, C. J., Huang, R., and Tang, R.: Characteristics and classification of landslide

- dams associated with the 2008 Wenchuan earthquake, *Geoenvironmental Disasters*, 4, 1-15, <https://doi.org/10.1186/s40677-017-0079-8>, 2017.
- 575 Fan, X., Yunus, A. P., Jansen, J. D., Dai, L., Strom, A., and Xu, Q.: Comment on ‘Gigantic rockslides induced by fluvial incision in the Diexi area along the eastern margin of the Tibetan Plateau’ by Zhao et al. (2019) *Geomorphology* 338, 27–42, *Geomorphology*, 402, <https://doi.org/10.1016/j.geomorph.2019.106963>, 2019.
- 580 Fan, X., Scaringi, G., Xu, Q., Zhan, W., Dai, L., Li, Y., Pei, X., Yang, Q., and Huang, R.: Coseismic landslides triggered by the 8th August 2017 Ms 7.0 Jiuzhaigou earthquake (Sichuan, China): factors controlling their spatial distribution and implications for the seismogenic blind fault identification, *Landslides*, 15, 967-983, <https://doi.org/10.1007/s10346-018-0960-x>, 2018.
- 585 Gao, H. S., Li, Z. M., Liu, F. L., Wu, Y. J., Li, P., Zhao, X., Li, F. Q., Guo, J., Liu, C. R., Pan, B. T., and Jia, H. T.: Terrace formation and river valley development along the lower Taohe River in central China, *Geomorphology*, 348, <https://doi.org/10.1016/j.geomorph.2019.106885>, 2020.
- Gao, X. and Li, Y.: Comparison on the incision rate in the upper and middle reaches of Minjiang River, *Resources and environment in the Yangtze Basin*, 15, 517-521, <https://doi.org/10.3969/j.issn.1004-8227.2006.04.020>, 2006.
- 590 Giano, S. I. and Giannandrea, P.: Late Pleistocene differential uplift inferred from the analysis of fluvial terraces (southern Apennines, Italy), *Geomorphology*, 217, 89-105, <https://doi.org/10.1016/j.geomorph.2014.04.016>, 2014.
- Gorum, T., Fan, X., van Westen, C. J., Huang, R. Q., Xu, Q., Tang, C., and Wang, G.: Distribution pattern of earthquake-induced landslides triggered by the 12 May 2008 Wenchuan earthquake, *Geomorphology*, 133, 152-167, <https://doi.org/10.1016/j.geomorph.2010.12.030>, 2011.
- 595 Grootes, P. M., Stulver, M., White, J. W. C., Johnsen, S. J., and Jouzel, J.: Comparison of oxygen records from the GISP2 and GRIP Greenland ice cores, *Nature*, 366, 6455, <https://doi.org/10.1038/366552a0>, 1993.
- 600 Guo, P.: Grain Size Characteristics and Optically stimulated luminescence Geochronology of Sediments in Diexi palaeo-dammed Lake, Upper Reaches of Minjiang River, China University of Geosciences, Beijing, 85 pp., 2018.
- Guo, X., Sun, Z., Lai, Z., Lu, Y., and Li, X.: Optical dating of landslide-dammed lake deposits in the upper Yellow River, Qinghai-Tibetan Plateau, China, *Quaternary International*, 392, 233-238, <https://doi.org/10.1016/j.quaint.2015.06.021>, 2016.
- 605 Hewitt, K.: Disturbance regime landscapes: mountain drainage systems interrupted by large rockslides, *Progress in Physical Geography: Earth and Environment*, 30, 365-393, <https://doi.org/10.1191/0309133306pp486ra>, 2016.
- Hewitt, K., Clague, J. J., and Orwin, J. F.: Legacies of catastrophic rock slope failures in mountain landscapes, *Earth-Science Reviews*, 87, 1-38, <https://doi.org/10.1016/j.earscirev.2007.10.002>, 2008.
- 610 Hewitt, K., Gosse, J., and Clague, J. J.: Rock avalanches and the pace of late Quaternary development of river valleys in the Karakoram Himalaya, *Geological Society of America Bulletin*, 123, 1836-1850, <https://doi.org/10.1130/b30341.1>, 2011.
- Hou, Z., Li, Z., Qu, X., Gao, Y., Hua, L., Zheng, M., Li, S., and Yuan, W.: The uplift process of the Qinghai-Tibet Plateau since 0.5Ma - Evidence from hot water activity in the Gangdese belt, *Science in China*, 31, 27-33, 2001.
- 615 Hu, H.-P., Feng, J.-L., and Chen, F.: Sedimentary records of a palaeo-lake in the middle Yarlung Tsangpo: Implications for terrace genesis and outburst flooding, *Quaternary Science Reviews*, 192, 135-148,

<https://10.1016/j.quascirev.2018.05.037>, 2018.

- Huang, Z., Tang, R., and Liu, S.: Re-discussion on the Jiaochang Arcuate Structure, Sichuan Province, and the Seismogenic Structure for Diexi Earthquake in 1933, *Earthquake Research in China*, 17, 51-62, <https://doi.org/CNKI:SUN:ZDZW.0.2003-01-005>, 2003.
- 620 Jansen, J. D., Fabel, D., Bishop, P., Xu, S., Schnabel, C., and Codilean, A. T.: Does decreasing paraglacial sediment supply slow knickpoint retreat?, *Geology*, 39, 543-546, <https://doi.org/10.1130/g32018.1>, 2011.
- Jansen, J. D., Nanson, G. C., Cohen, T. J., Fujioka, T., Fabel, D., Larsen, J. R., Codilean, A. T., Price, D. M., Bowman, H. H., May, J. H., and Gliganic, L. A.: Lowland river responses to intraplate tectonism and climate forcing quantified with luminescence and cosmogenic ¹⁰Be, *Earth and Planetary Science Letters*, 366, 49-58, <https://doi.org/10.1016/j.epsl.2013.02.007>, 2013.
- 625 Jiang, H., Zhong, N., Li, Y., Xu, H., Yang, H., and Peng, X.: Soft sediment deformation structures in the Lixian lacustrine sediments, eastern Tibetan Plateau and implications for postglacial seismic activity, *Sedimentary Geology*, 344, 123-134, <https://doi.org/10.1016/j.sedgeo.2016.06.011>, 2016.
- 630 Jiang, H., Mao, X., Xu, H., Yang, H., Ma, X., Zhong, N., and Li, Y.: Provenance and earthquake signature of the last deglacial Xinmocun lacustrine sediments at Diexi, East Tibet, *Geomorphology*, 204, 518-531, <https://doi.org/10.1016/j.geomorph.2013.08.032>, 2014.
- Kang, S., Wang, X., and Lu, Y.: Quartz OSL chronology and dust accumulation rate changes since the Last Glacial at Weinan on the southeastern Chinese Loess Plateau, *Boreas*, 42, 815-829, <https://10.1111/bor.12005>, 2013.
- 635 Kang, S., Du, J., Wang, N., Dong, J., Wang, D., Wang, X., Qiang, X., and Song, Y.: Early Holocene weakening and mid- to late Holocene strengthening of the East Asian winter monsoon, *Geology*, 48, 1043-1047, <https://10.1130/g47621.1>, 2020.
- 640 Kaplan, M. R., Wolfe, A. P., and Miller, G. H.: Holocene Environmental Variability in Southern Greenland Inferred from Lake Sediments, *Quaternary Research*, 58, 149-159, <https://doi.org/10.1006/qres.2002.2352>, 2002.
- Keaveney, E. M. and Reimer, P. J.: Understanding the variability in freshwater radiocarbon reservoir offsets: a cautionary tale, *Journal of Archaeological Science*, 39, 1306-1316, <https://doi.org/10.1016/j.jas.2011.12.025>, 2012.
- 645 Kirby, E., Whipple, K. X., Burchfiel, B. C., Tang, W., Berger, G., Sun, Z., and Chen, Z.: Neotectonics of the Min Shan, China: Implications for mechanisms driving Quaternary deformation along the eastern margin of the Tibetan Plateau, *Geological Society of America Bulletin*, 112, 375-393, [https://doi.org/10.1130/0016-7606\(2000\)112<375:NOTMSC>2.0.CO;2](https://doi.org/10.1130/0016-7606(2000)112<375:NOTMSC>2.0.CO;2), 2000.
- 650 Korup, O. and Montgomery, D. R.: Tibetan plateau river incision inhibited by glacial stabilization of the Tsangpo gorge, *Nature*, 455, 786-789, <https://doi.org/10.1038/nature07322>, 2008.
- Korup, O., Densmore, A. L., and Schlunegger, F.: The role of landslides in mountain range evolution, *Geomorphology*, 120, 77-90, <https://doi.org/10.1016/j.geomorph.2009.09.017>, 2010.
- Korup, O., Clague, J. J., Hermanns, R. L., Hewitt, K., Strom, A. L., and Weidinger, J. T.: Giant landslides, topography, and erosion, *Earth and Planetary Science Letters*, 261, 578-589, <https://doi.org/10.1016/j.epsl.2007.07.025>, 2007.
- 655 Krivonogov, S. K., Takahara, H., Kuzmin, Y. V., Orlova, L. A., Timothy Jull, A. J., Nakamura, T., Miyoshi, N., Kawamuro, K., and Bezrukova, E. V.: Radiocarbon Chronology of the Late Pleistocene–Holocene Paleogeographic Events in Lake Baikal Region (Siberia), *Radiocarbon*, 46, 745-754, <https://doi.org/10.1017/s0033822200035785>, 2016.
- 660

- Li, J. and Fang, X.: Study on the uplift and environmental change of the Qinghai-Tibet Plateau, Chinese Science Bulletin, 43, 1563-1574, <https://doi.org/CNKI:SUN:KXTB.0.1998-15-000>, 1998.
- 665 Liu, Y., Wang, X., Su, Q., Yi, S., Miao, X., Li, Y., and Lu, H.: Late Quaternary terrace formation from knickpoint propagation in the headwaters of the Yellow River, NE Tibetan Plateau, Earth Surface Processes and Landforms, 46, 2788-2806, <https://doi.org/10.1002/esp.5208>, 2021.
- Lu, H., An, Z., Wang, X., Tan, H., Zhu, R., Ma, H., Li, Zhen, Miao, X., and Wang, X.: The staged uplift of the northeastern margin of the Qinghai-Tibet Plateau in the recent 14 Ma Geomorphic evidence, Science in China Series D Earth Sciences, 34, 855-864, <https://doi.org/10.3321/j.issn:1006-9267.2004.09.008>, 2004.
- 670 Luo, X., Yin, Z., and Yang, L.: Preliminary analysis on the development characteristics of river terraces and their relationship with ancient landslides in the upper reaches of Minjiang River, Quaternary Sciences, 39, 391-398, <https://doi.org/10.11928/j.issn.1001-7410.2019.02.11>, 2019.
- Ma, J.: Sedimentary Characteristics of Outburst Deposits and Inversion of Outburst Flood Induced by the Diexi Paleo Dammed Lake of the Upper Minjiang River in China, China University of Geosciences, Beijing, 97 pp., 2017.
- 675 Ma, J., Chen, J., Cui, Z., Zhou, W., Liu, C., Guo, P., and Shi, Q.: Sedimentary evidence of outburst deposits induced by the Diexi paleo-landslide-dammed lake of the upper Minjiang River in China, Quaternary International, 464, 460-481, <https://doi.org/10.1016/j.quaint.2017.09.022>, 2018.
- Malatesta, L. C. and Avouac, J.-P.: Contrasting river incision in north and south Tian Shan piedmonts due to variable glacial imprint in mountain valleys, Geology, 46, 659-662, 10.1130/g40320.1, 2018.
- 680 Malatesta, L. C., Finnegan, N. J., Huppert, K. L., and Carreño, E. I.: The influence of rock uplift rate on the formation and preservation of individual marine terraces during multiple sea-level stands, Geology, 50, 101-105, <https://doi.org/10.1130/g49245.1>, 2021.
- Mao, X.: Preliminary study on lacustrine sediments at Diexi in the upper reach of the Minjiang River during the last deglaciation, China university of Geosciences, Beijing, 71 pp., 2011.
- 685 Miall, A. D.: Principles Of Sedimentary Basin, Springer, 616 pp.2000.
- Molnar, P. and Houseman, G. A.: Rayleigh-Taylor instability, lithospheric dynamics, surface topography at convergent mountain belts, and gravity anomalies, Journal of Geophysical Research: Solid Earth, 118, 2544-2557, <https://doi.org/10.1002/jgrb.50203>, 2013.
- 690 Molnar, P., England, P., and Martinod, J.: Mantle dynamics, uplift of the Tibetan Plateau, and the Indian monsoon, Journal of Geophysical Research: Solid Earth, 118, 2544-2557, <https://doi.org/10.1029/93RG02030>, 1993.
- Montgomery, D. R., Hallet, B., Yuping, L., Finnegan, N., Anders, A., Gillespie, A., and Greenberg, H. M.: Evidence for Holocene megafloods down the tsangpo River gorge, Southeastern Tibet, Quaternary Research, 62, 201-207, <https://10.1016/j.yqres.2004.06.008>, 2004.
- 695 Murray, A. S. and Wintle, A. G.: Luminescence dating of quartz using an improved single-aliquot regenerative-dose protocol, Radiation Measurements, 32, 57-73, [https://doi.org/10.1016/S1350-4487\(99\)00253-X](https://doi.org/10.1016/S1350-4487(99)00253-X), 2000.
- Oh, J. S., Seong, Y. B., Hong, S., and Yu, B. Y.: Paleo-shoreline changes in moraine dammed lake Khagiin Khar, Khentey Mountains, Central Mongolia, Journal of Mountain Science, 16, 1215-1230, <https://doi.org/10.1007/s11629-019-5445-4>, 2019.
- 700 Okuno, J., Nakada, M., Ishii, M., and Miura, H.: Vertical tectonic crustal movements along the Japanese coastlines inferred from late Quaternary and recent relative sea-level changes, Quaternary Science Reviews, 91, 42-61, <https://doi.org/10.1016/j.quascirev.2014.03.010>, 2014.

- 705 Pan, B., Burbank, D., Wang, Y., Wu, G., Li, J., and Guan, Q.: A 900 k.y. record of strath terrace formation during glacial-interglacial transitions in northwest China, *Geology*, 31, <https://doi.org/10.1130/g19685.1>, 2003.
- Pan, B., Hu, X., Gao, H., Hu, Z., Cao, B., Geng, H., and Li, Q.: Late Quaternary river incision rates and rock uplift pattern of the eastern Qilian Shan Mountain, China, *Geomorphology*, 184, 84-97, <https://doi.org/10.1016/j.geomorph.2012.11.020>, 2013.
- 710 Prescott, J. R. and Hutton, J. T.: Cosmic ray contributions to dose rates for luminescence and ESR dating: large depths and long-term time variations, *Radiation Measurements*, 23, 497-500, [https://doi.org/10.1016/1350-4487\(94\)90086-8](https://doi.org/10.1016/1350-4487(94)90086-8), 1994.
- Rees-Jones, J.: Optical dating of young sediments using fine-grain quartz, *Ancient TL*, 13, 9-14, 1995.
- 715 Reimer, P. J., Austin, W. E. N., Bard, E., Bayliss, A., Blackwell, P. G., Bronk Ramsey, C., Butzin, M., Cheng, H., Edwards, R. L., Friedrich, M., Grootes, P. M., Guilderson, T. P., Hajdas, I., Heaton, T. J., Hogg, A. G., Hughen, K. A., Kromer, B., Manning, S. W., Muscheler, R., Palmer, J. G., Pearson, C., van der Plicht, J., Reimer, R. W., Richards, D. A., Scott, E. M., Southon, J. R., Turney, C. S. M., Wacker, L., Adolphi, F., Büntgen, U., Capano, M., Fahrni, S. M., Fogtmann-Schulz, A., Friedrich, R., Köhler, P., Kudsk, S., Miyake, F., Olsen, J., Reinig, F., Sakamoto, M., Sookdeo, A., and Talamo, S.: The IntCal20 Northern Hemisphere Radiocarbon Age Calibration Curve (0–55 cal kBP), *Radiocarbon*, 62, 725-757, <https://doi.org/10.1017/rdc.2020.41>, 2020.
- Schumm, S. A. and Parker, R. S.: Implications of Complex Response of Drainage Systems for Quaternary Alluvial Stratigraphy, *Nature*, 243, 99-100, <https://doi.org/10.1038/physci243099a0>, 1973.
- 725 Shi, W.: Impact of tectonic activities and climate change on the lacustrine sediments in the eastern Tibet during the last deglaciation, Institute of Geology, China Earthquake Administrator, Beijing, 135 pp., 2020.
- Shi, Y., Li, J., Li, B., Yao, T., Wang, S., Li, S., Cui, Z., Wang, F., Pan, B., Fang, X., and Zhang, Q.: Uplift of the Qinghai—Xizang (Tibetan) Plateau and east Asia environmental change during late cenozoic, *ACTA GEOGRAPHICA SINICA*, 12-22, <https://doi.org/10.3321/j.issn:0375-5444.1999.01.002>, 1999.
- 730 Singh, A. K., Pattanaik, J. K., Gagan, and Jaiswal, M. K.: Late Quaternary evolution of Tista River terraces in Darjeeling-Sikkim-Tibet wedge: Implications to climate and tectonics, *Quaternary International*, 443, 132-142, <https://doi.org/10.1016/j.quaint.2016.10.004>, 2017.
- 735 Srivastava, P., Tripathi, J. K., Islam, R., and Jaiswal, M. K.: Fashion and phases of late Pleistocene aggradation and incision in the Alaknanda River Valley, western Himalaya, India, *Quaternary Research*, 70, 68-80, <https://doi.org/10.1016/j.yqres.2008.03.009>, 2017.
- Tang, R., Jiang, N., and Liu, S.: Recognition of the Geological Setting and the Seismogenic Condition for the Diexi Magnitude 7.5 Earthquake, *Journal of seismological research*, 6, 327-338, <https://doi.org/CNKI:SUN:DZYJ.0.1983-03-011>, 1983.
- 740 Tian, Q., Kirby, E., Zheng, W., Zhang, H., Liang, H., Li, Z., Wang, W., Li, T., Zhang, Y., Xu, B., and Zhang, P.: Late Quaternary variations in paleoerosion rates in the northern Qilian Shan revealed by ¹⁰Be in fluvial terraces, *Geomorphology*, 386, 10.1016/j.geomorph.2021.107751, 2021.
- 745 Vásquez, A., Flores-Aqueveque, V., Sagredo, E., Hevia, R., Villa-Martínez, R., Moreno, P. I., and Antinao, J. L.: Evolution of Glacial Lake Cochrane During the Last Glacial Termination, Central Chilean Patagonia (~47°S), *Frontiers in Earth Science*, 10, 1-19, <https://doi.org/10.3389/feart.2022.817775>, 2022.
- Wang, H., Wang, P., Hu, G., Ge, Y., and Yuan, R.: An Early Holocene river blockage event on the western

- boundary of the Namche Barwa Syntaxis, southeastern Tibetan Plateau, *Geomorphology*, 395, 1-20,
750 <https://doi.org/10.1016/j.geomorph.2021.107990>, 2021.
- Wang, L., Wang, X., Xu, X., and Cui, J.: What happened on the upstream of Minjiang River in Sichuan
Province 20,000 years ago, *Earth Science Frontiers*, 14, 189-196,
<https://www.earthsciencefrontiers.net.cn/CN/Y2007/V14/I6/189>, 2007.
- Wang, L., Yang, L., Wang, X., and Duan, L.: Discovery of huge ancient dammed lake on upstream of
755 Minjiang River in Sichuan , China, *Journal of Chengdu University of Technology (Science &
Technology Edition)*, 32, 1-11, <https://doi.org/CNKI:SUN:CDLG.0.2005-01-001>, 2005a.
- Wang, L., Yang, L., Wang, X., and Duan, L.: Discovery of huge ancient dammed lake on upstream of
Minjiang River in Sichuan , China, *Journal of Chengdu University of Technology*, 32, 1-11, 2005b.
- Wang, L., Wang, X., Xu, X., Cui, J., Shen, J., and Zhang, Z.: Significances of studying the diexi paleo
760 dammed lake at the upstream of minjiang river, sichuan, China, *Quaternary Sciences*, 32, 998-1010,
<https://doi.org/10.3969/j.issn.1001-7410.2012.05.16>, 2012.
- Wang, L., Wang, X., Shen, J., Xu, X., Cui, J., Zhang, Z., and Zhou, Z.: The effect of evolution of Diexi
ancient barrier lake in the upper Mingjiang River on the Chengdu Plain in Sichuan, China, *Journal
of Chengdu University of technology*, 47, 1-15, [https://doi.org/10.3969/j.issn.1671-
9727.2020.01.01](https://doi.org/10.3969/j.issn.1671-9727.2020.01.01), 2020a.
- 765 Wang, L., Wang, X., Shen, J., Yin, G., Cui, J., Xu, X., Zhang, Z., Wan, T., and Wen, L.: Late Pleistocene
environmental information on the Diexi paleo-dammed lake of the upper Minjiang River in the
eastern margin of the Tibetan Plateau, China, *Journal of Mountain Science*, 17, 1172-1187,
<https://10.1007/s11629-019-5573-x>, 2020b.
- 770 Wang, P., Zhang, B., Qiu, W., and Wang, J.: Soft-sediment deformation structures from the Diexi paleo-
dammed lakes in the upper reaches of the Minjiang River, east Tibet, *Journal of Asian Earth Sciences*,
40, 865-872, <https://doi.org/10.1016/j.jseaes.2010.04.006>, 2011.
- Wang, X.: The Environment Geological Information in the Sediments of Diexi Ancient Dammed Lake
on the upstream of Mingjiang River in Sichuan Province, China, Chengdu University of Technology,
775 Chengdu, 116 pp., 2009.
- Wang, X., Li, Y., Yuan, Y., Zhou, Z., and Wang, L.: Palaeoclimate and palaeoseismic events discovered
in Diexi barrier lake on the Minjiang River, China, *Natural Hazards and Earth System Sciences*, 14,
2069-2078, <https://doi.org/10.5194/nhess-14-2069-2014>, 2014.
- 780 Wang, Y., Cheng, H., Edwards, R. L., An, Z., Wu, J., Shen, C.-C., and Dorale, J. A.: A high-resolution
absolute-dated late Pleistocene monsoon record from Hulu cave, China, *Science*, 294, 2345-2348,
<https://doi.org/10.1126/science.1064618>, 2001.
- Wang, Y., Cheng, H., Edwards, R. L., Kong, X., Shao, X., Chen, S., Wu, J., Jiang, X., Wang, X., and
Wang, Z.: Millennial- and orbital-scale changes in the East Asian monsoon over the past 224,000
years, *Nature*, 451, 1090-1093, <https://doi.org/10.1038/nature06692>, 2008.
- 785 Westaway, R. and Bridgland, D.: Late Cenozoic uplift of southern Italy deduced from fluvial and marine
sediments: Coupling between surface processes and lower-crustal flow, *Quaternary International*,
175, 86-124, <https://doi.org/10.1016/j.quaint.2006.11.015>, 2007.
- Wintle, A. G. and Murray, A. S.: A review of quartz optically stimulated luminescence characteristics
and their relevance in single-aliquot regeneration dating protocols, *Radiation Measurements*, 41,
790 369-391, <https://10.1016/j.radmeas.2005.11.001>, 2006.
- Wu, L., Zhao, D. J., Zhu, J., Peng, J., and Zhou, Y.: A Late Pleistocene river-damming landslide, Minjiang
River, China, *Landslides*, 17, 433-444, <https://doi.org/10.1007/s10346-019-01305-5>, 2019.

- Xu, H., Chen, J., Cui, Z., and Chen, R.: Sedimentary facies and depositional processes of the Diexi Ancient Dammed Lake, Upper Minjiang River, China, *Sedimentary Geology*, 398, <https://doi.org/10.1016/j.sedgeo.2019.105583>, 2020.
- 795 Yang, F., Fan, X., Siva Subramanian, S., Dou, X., Xiong, J., Xia, B., Yu, Z., and Xu, Q.: Catastrophic debris flows triggered by the 20 August 2019 rainfall, a decade since the Wenchuan earthquake, China, *Landslides*, 18, 3197-3212, <https://doi.org/10.1007/s10346-021-01713-6>, 2021.
- Yang, N., Zhang, Y., Meng, H., and Zhang, H.: Study of the Minjiang River terraces in the western Sichuan Plateau, *Journal of Geomechanics*, 9, 363-370, <https://doi.org/10.3969/j.issn.1006-6616.2003.04.008>, 2003.
- 800 Yang, W.: Research of Sedimentary Record in Terraces and Climate Vary in the Upper Reaches of Minjiang River, China, Chengdu University of Technology, Chengdu, 2005.
- Yang, W., Zhu, L., Zhang, Y., and Kan, A.: Sedimentary evolution of a dammed paleolake in the Maoxian basin on the upper reach of Minjiang River, Sichuan, China, *Marine Geology Frontiers*, 27, 35-40, <https://doi.org/CNKI:SUN:HYDT.0.2011-05-007>, 2011.
- 805 Yang, W., Zhu, L., Zheng, H., Xiang, F., Kan, A., and Luo, L.: Evoluton of a dammed palaeolake in the Quaternary Diexi basin on the upper Minjiang River, Sichuan, China, *Geological Bulletin of China*, 27, 605-610, <https://doi.org/10.3969/j.issn.1671-2552.2008.05.003>, 2008.
- 810 Yang, Y., Li, B., Yin, Z., and Zhang, Q.: The Formation and Evolution of Landforms in the Xizang Plateau, *ACTA GEORAPHICA SINICA*, 76-87, <https://doi.org/10.11821/xb198201009>, 1982.
- Yoshikawa, T., KaizukaYoko, S., and Ota, O.: Mode of crustal movement in the late Quaternary on the southeast coast of Shikoku, southwestern Japan, *Geographical Review of Japan*, 37, 627-648, <https://doi.org/10.4157/grj.37.627>, 1964.
- 815 Yu, Y., Wang, X., Yi, S., Miao, X., Vandenberghe, J., Li, Y., and Lu, H.: Late Quaternary aggradation and incision in the headwaters of the Yangtze River, eastern Tibetan Plateau, China, *GSA Bulletin*, 134, 371-388, <https://doi.org/10.1130/b35983.1>, 2021.
- Yuan, G. and Zeng, Q.: Glacier-dammed lake in Southeastern Tibetan Plateau during the Last Glacial Maximum, *Journal Geological Society of India*, 79, 295-301, <https://doi.org/10.1007/s12594-012-0041-z>, 2012.
- 820 Zhang, B., Wang, P., and Wang, J.: Discussion of the Origin of the Soft-Sediment Deformation Structures in Paleo-dammed Lake Sediments in the Upper Reaches of the Minjiang River, *Journal of Seismological Research*, 34, 67-74, <https://doi.org/10.3969/j.issn.1000-0666.2011.01.011>, 2011.
- Zhang, S.: Characteristics and Geological Significance of the Late Pleistocene Lacustrine Sediments in Diexi, Sichuan, China University of Geosciences, Beijing, 76 pp., 2019.
- 825 Zhang, Y., Zhu, L., Yang, W., Luo, H., Jiang, L., He, D., and Liu, J.: High Resolution Rapid Climate Change Records of Lacustrine Deposits of Diexi Basin in the Eastern Margin of Qinghai-Tibet Plateau, 40–30 ka BP, *Earth Science Frontiers*, 16, 91-98, [https://doi.org/10.1016/s1872-5791\(08\)60106-2](https://doi.org/10.1016/s1872-5791(08)60106-2), 2009.
- 830 Zhao, X., Deng, Q., and Chen, S.: Tectonic geomorphology of the Minshan uplift in western Sichuan, southwestern China, *Seismology and Geology*, 16, 429-439, <https://doi.org/CNKI:SUN:DZDZ.0.1994-04-017>, 1994.
- Zhong, N.: Earthquake and Provenance Analysis of the Lacustrine Sediments in the Upper Reaches of the Min River during the Late Pleistocene, Institute of Geology, China Earthquake Administration, Beijing, 193 pp., 2017.
- 835 Zhong, Y., Fan, X., Dai, L., Zou, C., Zhang, F., and Xu, Q.: Research on the Diexi Giant Paleo-Landslide

along Minjiang River in Sichuan, China, *Progress in Geophysics*, 36, 1784-1796,
<https://doi.org/10.6038/pg2021EE0367>, 2021.

840 Zhou, R., Pu, X., He, Y., Li, X., and Ge, T.: Recent activity of Minjiang fault zone, uplift of Minshan
block and their relationship with seismicity of Sichuan, *Seismology and Geology*, 22, 285-294,
<https://doi.org/CNKI:SUN:DZDZ.0.2000-03-009>, 2000.

Zhu, J.: A preliminary study on the upper reaches of Minjiang River Terrace, Chengdu University of
Technology, Chengdu, 73 pp., 2014.

845 Zhu, S., Wu, Z., Zhao, X., and Keyan, X.: Glacial dammed lakes in the Tsangpo River during late
Pleistocene, southeastern Tibet, *Quaternary International*, 298, 114-122,
<https://10.1016/j.quaint.2012.11.004>, 2013.